MDPI

Article

Silver Nanoparticles Synthesized from *Abies alba* and *Pinus sylvestris* Bark Extracts: Characterization, Antioxidant, Cytotoxic, and Antibacterial Effects

Irina Macovei [1], Simon Vlad Luca [2], Krystyna Skalicka-Woźniak [3], Cristina Elena Horhogea [4,*], Cristina Mihaela Rimbu [4], Liviu Sacarescu [5], Gabriela Vochita [6], Daniela Gherghel [6], Bianca Laura Ivanescu [1], Alina Diana Panainte [1], Constantin Nechita [7], Andreia Corciova [1] and Anca Miron [1,*]

1   Faculty of Pharmacy, Grigore T. Popa University of Medicine and Pharmacy, 700115 Iasi, Romania
2   Biothermodynamics, TUM School of Life Sciences, Technical University of Munich, D-85354 Freising, Germany
3   Department of Natural Products Chemistry, Medical University of Lublin, 20-093 Lublin, Poland
4   Department of Public Health, Ion Ionescu de la Brad University of Life Sciences, 700489 Iasi, Romania
5   Petru Poni Institute of Macromolecular Chemistry, 700487 Iasi, Romania
6   NIRDBS, Institute of Biological Research Iasi, 700107 Iasi, Romania
7   Marin Dracea National Institute for Research and Development in Forestry, 725100 Campulung Moldovenesc, Romania
*   Correspondence: chorhogea@uaiasi.ro (C.E.H.); anca.miron@umfiasi.ro (A.M.)

Abstract: In recent years, phytofunctionalized AgNPs have attracted great interest due to their remarkable biological activities. In the present study, AgNPs were synthesized using *Abies alba* and *Pinus sylvestris* bark extracts. The chemical profile of these bark extracts was analyzed by LC-HRMS/MS. As a first step, the synthesis parameters (pH, AgNO$_3$ concentration, ratio of bark extract and AgNO$_3$, temperature, and reaction time) were optimized. The synthesized AgNPs were characterized by ATR-FTIR spectroscopy, DLS, SEM, EDX, and TEM. Their antioxidant, cytotoxic, and antibacterial properties were evaluated by the DPPH, ABTS, MTT, and broth microdilution assays, respectively. *Abies alba* and *Pinus sylvestris* bark extract-derived AgNPs were well-dispersed, spherical, small (average particle size of 9.92 and 24.49 nm, respectively), stable (zeta potential values of −10.9 and −10.8 mV, respectively), and cytotoxic to A-375 human malignant melanoma cells (IC$_{50}$ = 2.40 ± 0.21 and 6.02 ± 0.61 µg/mL, respectively). The phytosynthesized AgNPs also showed antioxidant and antibacterial effects.

Keywords: phytofunctionalized silver nanoparticles; bark extract; *Abies alba* Mill.; *Pinus sylvestris* L.; A-375 human melanoma cells; DPPH scavenging activity; ABTS scavenging activity; antibacterial activity

check for updates

1. Introduction

Among nanomaterials, silver nanoparticles (AgNPs) have gained increasing attention over the last years due to their strong antimicrobial activity and unique electrical, optical, and catalytic properties. Nowadays, AgNPs have been imposed as a desirable nanomaterial in different fields such as medicine (impregnation of catheters, meshes for wounds and tissue therapy, bone and cardiovascular implants, bio-imaging, bio-sensing), cosmetics, food preservation, environmental protection (water disinfection), paint coating industry, and catalysis of various processes [1]. Many of the biomedical applications of AgNPs are based on their broad-spectrum antimicrobial activity against bacteria, fungi, and viruses [2]. AgNPs exert higher toxicity against Gram-negative bacteria which is strongly related to the thinner peptidoglycan layer in the bacterial cell wall [3,4]. AgNPs are also active against drug-resistant bacteria, enhance the antibacterial activity of antibiotics [4], have

antitumor properties, inhibit angiogenesis, and increase chemosensitivity in multidrug-resistant cancer cells [5,6].

The bioactivity of AgNPs can be enhanced and/or enlarged by phytofunctionalization. This can be achieved by using plant extracts to synthesize AgNPs. Phytochemicals present in plant extracts have multiple functions: they reduce Ag^+ to metallic Ag and stabilize and modulate the activity of AgNPs [7,8]. The use of the aqueous extracts of *Hemidesmus indicus* roots and *Mikania cordata* leaves in the synthesis of AgNPs resulted in strong antibacterial activity against Gram-positive *Staphylococcus aureus* and potent cytotoxicity against PA-1 ovarian cancer cell line [9,10]. AgNPs synthesized using the soap nuts (*Sapindus* sp.) aqueous extract showed higher toxicity against Gram-positive bacteria (*S. aureus*) than Gram-negative bacteria (*Escherichia coli, Pseudomonas aeruginosa*) [11]. Phytofunctionalized AgNPs, active against both Gram-positive and Gram-negative bacteria, were obtained using extracts of *Diospyros paniculata* and *Diospyros sylvatica* roots, *Acorus calamus* rhizome, *Cucurbita maxima* petals, *Moringa oleifera, Azadirachta indica, Sesbania grandiflora, Ginkgo biloba, Carica papaya*, and *Nigella arvensis* leaves, *Coffea arabica* seeds, and cacao [2,12]. Phytofunctionalized AgNPs have also noticeable antioxidant effects conferred by both elemental Ag and phytochemicals capping AgNPs, the plant extract concentration and antioxidant potential of phytofunctionalized AgNPs being positively correlated [13]. AgNPs synthesized using the aqueous extract of *Allium cepa* bulbs showed promising effects for the treatment of diabetes: inhibition of enzymes involved in carbohydrate metabolism (α-amylase, α-glucosidase) and antioxidant activity but low cytotoxicity against 3T3 pre-adipocytes [14]. AgNPs obtained using the ethanolic extract of *Tabernaemontana divaricata* leaves prevented sodium selenite-induced cataractogenesis in in vitro and in vivo models. In vitro AgNPs attenuated the oxidative stress (decrease in reduced glutathione and activity of antioxidant enzymes, increase in malondialdehyde) in lenses exposed to sodium selenite, thus impeding lens opacification [15]. In selenite-challenged Wistar rat pups, the same AgNPs prevented cataractogenesis by maintaining calcium homeostasis (regulation of lenticular ATPases activity, regulation of genes encoding calcium transporter proteins) which is essential for the integrity of lenticular structural and cytoskeletal proteins. In the same study, chemically synthesized AgNPs showed insignificant anticataractogenic effects [16]. AgNPs synthesized using an aqueous extract of *Turbinaria conoides*, a brown seaweed, showed heart and liver regeneration effects in zebrafish (*Danio rerio*) as revealed by histological studies [17]. Overall, in contrast to "naked" AgNPs, the phytofunctionalized ones have important advantages such as improved bioactivity, higher stability, and reduced toxicity [18].

Coniferous plants, consisting of 8 families, 70 genera, and 630 species distributed worldwide, represent an important source of bioactive phytochemicals (polyphenols, terpenoids, alkaloids) and therefore, they are good candidates for the phytosynthesis of AgNPs [19,20]. Extracts obtained from different parts of coniferous trees (bark, needles, cones, twigs, heart wood, berries) were reported to exhibit various biological effects (antioxidant, anti-inflammatory, anticancer, antimicrobial, analgesic, antidiabetic, anticonvulsant), some extracts being commercially available on the market [20].

Abies alba Mill. (Pinaceae, silver fir) and *Pinus sylvestris* L. (Pinaceae, Scots pine) are important timber trees in Romania, the bark being the main by-product of the industrial processing of the wood [21,22]. Previous investigations on *A. alba* bark extracts in cell-free and cell-based assays revealed antioxidant (free radical scavenging activity, decrease of the production of reactive oxygen species, reduction of lipoprotein oxidation) [22–24], anti-steatotic (decrease of lipid and cholesterol accumulation in hepatocytes, slight induction of cholesterol conversion to bile acids), and antihypertensive (inhibition of angiotensin-converting enzyme) effects [24]. *P. sylvestris* bark extracts were reported to display anti-inflammatory activity (reduction of the synthesis of pro-inflammatory prostaglandin E_2 and nitric oxide) in murine macrophages [25], pro-apoptotic effects in human cervical adenocarcinoma (HeLa) cells [21], antiparasitic activity against *Cryptosporidium parvum*, responsible for severe diarrhoeal disease [26], antibacterial activity against *S. aureus*, in-

cluding a methicillin-resistant strain, and free radical scavenging activity [27]. To the best of our knowledge, there is no report on the phytosynthesis of AgNPs from *A. alba* or *P. sylvestris* bark extracts. Therefore, this study was designed to synthesize AgNPs by using the aqueous extracts of *A. alba* and *P. sylvestris* bark, to characterize the synthesized AgNPs, and to investigate their antioxidant, cytotoxic, and antibacterial properties.

2. Materials and Methods

2.1. Plant Material

A. alba and *P. sylvestris* bark fragments were collected from mature trees (35–40 years old, 18–25 cm circumference at breast height) in Suceava county (47°45′13″ N, 26°12′19″ E), Romania, in March 2018. Species authentication was performed by Dr. Constantin Nechita (Forest Research and Management Institute, Campulung Moldovenesc, Suceava, Romania). Voucher specimens (AA1520/2018, PS1517/2018) are deposited in the Department of Pharmacognosy-Phytotherapy, Faculty of Pharmacy, Grigore T. Popa University of Medicine and Pharmacy, Iasi, Romania. Bark pieces were washed with distilled and then ultra-pure water, chopped, dried in a dark room at 20 ± 2 °C, powdered, and stored at +4 °C until extraction.

2.2. Chemicals and Reagents

Ciprofloxacin hydrochloride, Folin–Ciocalteu's phenol reagent, gallic acid, sodium carbonate, formic acid (HPLC), acetonitrile (HPLC), 2,2-diphenyl-1-picrylhydrazyl (DPPH) radical, 2,2′-azinobis(3-ethylbenzothiazoline-6-sulfonic acid) diammonium salt (ABTS), (R)-(+)-6-hydroxy-2,5,7,8-tetramethylchroman-2-carboxylic acid (Trolox), silver nitrate ($AgNO_3$), and dimethyl sulfoxide (DMSO) were purchased from Sigma-Aldrich (Steinheim, Germany). 3-(4,5-Dimethyl-2-thiazolyl)-2,5-diphenyl-2H-tetrazolium bromide (MTT) was obtained from Merck (Darmstadt, Germany). Dulbecco's Modified Eagle's Medium/Dulbecco's Minimum Essential Media (DMEM) and penicillin-streptomycin solution were purchased from Biological Industries Israel Beit Haemek Ltd. (Beit Haemek, Israel). Mueller-Hinton broth was supplied by Oxoid (Basingstoke, UK). Fetal bovine serum and trypsin/ethylenediaminetetraacetic acid (EDTA) solution were provided by Biochrom (Berlin, Germany). All other chemicals and reagents were of analytical grade. Ultra-pure water was obtained from SG Water Ultra Clear TWF water purification system (Barsbüttel, Germany).

2.3. Microorganisms

Staphylococcus aureus ATCC 25923 and ATCC 43300, *Staphylococcus epidermidis* ATCC 12228, *Escherichia coli* ATCC 25922, and *Pseudomonas aeruginosa* ATCC 9027 were purchased from the American Type Culture Collection (ATCC, Manassas, VA, USA).

2.4. Cell Lines

African green monkey kidney (Vero, ATCC® CCL-81™) and human malignant melanoma (A-375, ATCC® CRL-1619™) cell lines were procured from ATCC (Manassas, VA, USA).

2.5. Preparation of Bark Extracts

Extraction was performed with ultra-pure water at a ratio of 1:10 as previously described. Briefly, bark powder (10 g) was mixed with ultra-pure water (100 mL) at 60 °C followed by 3 h stirring at room temperature, filtration, and addition of ultra-pure water to 100 mL final volume [28,29].

2.6. Chemical Characterization of Bark Extracts

2.6.1. Qualitative Analysis of Bark Extracts

The chemical profile of bark extracts was analyzed by liquid chromatography hyphenated with high-resolution tandem mass spectrometry (LC-HRMS/MS). The analysis was performed on an Agilent 1200 HPLC system (Agilent Technologies, Santa Clara, California, USA) equipped with auto-sampler (G1329B), degasser (G1379B), binary pump

(G1312C), thermostat (G1316A), diode array detector (G1315D), Agilent ESI-Q-TOF mass spectrometer (G6530B), nitrogen generator (Parker Hannifin Corp., Cleveland, OH, USA), and compressed air generator (Jun-Air Oxymed, Łódź, Poland). The chromatographic separations were performed as previously described [29,30] with minor changes: column: Phenomenex Gemini C18 (2 × 100 mm, 3 µm), column temperature 20 °C, mobile phase: 0.1% formic acid in water (A) and 0.1% formic acid in acetonitrile (B), elution gradient: 0 min: 5% B, 0–45 min: 5–60% B, 45–55 min: 60–95% B, flow rate 0.2 mL/min, and injection volume: 10 µL. The following MS parameters were used: negative ionization mode, *m/z* range 70–1000, gas (N_2) temperature 275 °C, N_2 flow 10 L/min, nebulizer 35 psi, sheath gas temperature 325 °C, sheath gas flow rate 12 L/min, capillary voltage 4000 V, nozzle voltage 1000 V, skimmer 65 V, fragmentor 140 V, fixed collision-induced dissociation energies 10 and 30 V. MassHunter Qualitative Analysis Navigator B.08.00 software (Agilent) was used for data processing.

2.6.2. Quantitative Analysis of Bark Extracts

The total phenolic content in bark extracts was quantified using the Folin–Ciocalteu method. In summary, the reaction mixture consisted of a sample (0.04 mL), ultra-pure water (3.16 mL), Folin–Ciocalteu's phenol reagent (0.2 mL), and 20% sodium carbonate (0.6 mL). After 2 h incubation at room temperature, the absorbance was determined at 765 nm (Specord 210 Plus spectrophotometer, Analytik Jena, Jena, Thuringia, Germany). The phenolic content was expressed as gallic acid equivalents (µg/mL) [31,32]. The assay was carried out in triplicate.

The total phenolic content was also determined in the reaction mixtures (bark aqueous extract and 2 mM $AgNO_3$, 1:9, *v/v*) before and after the synthesis and separation of AgNPs.

2.7. Synthesis of AgNPs

The synthesis of AgNPs was monitored and optimized by recording the UV-Vis spectra of the reaction mixtures in the wavelength range of 350–800 nm [29,33–36] on a Specord 210 Plus spectrophotometer (Analytik Jena, Jena, Thuringia, Germany). In order to obtain the maximum yield of AgNPs, the synthesis was conducted at various parameters such as pH value of the reaction mixture (2, 4, 6, 8, and 10), $AgNO_3$ concentration (0.5, 1, 2, and 3 mM), ratio of aqueous bark extract and $AgNO_3$ (1:9, 2:8, 5:5, 7:3, and 9:1, *v/v*), temperature (30, 40, 50, 60, 70, and 80 °C), and reaction time (10, 20, 30, 60, and 120 min). HCl (0.1 N) and NaOH (0.1 N) were used to adjust the pH of the reaction mixture. Once the optimization studies were completed, the synthesis of AgNPs was conducted using the optimal parameters. The dispersed AgNPs were further separated by centrifugation at 9000 rpm for 20 min (Hettich Rotina 380 R centrifuge, Hettich, Tuttlingen, Germany), washed 5 times with ultra-pure water to remove the unreacted material, and finally freeze-dried (Unicryo TFD 5505 freeze dryer, UniEquip GmbH, Munich, Germany). The AgNPs pellets were stored at +4 °C until use.

2.8. Characterization of AgNPs

AgNPs were characterized by attenuated total reflection Fourier-transform infrared (ATR-FTIR) spectroscopy, dynamic light scattering (DLS), scanning electron microscopy (SEM), energy dispersive X-ray analysis (EDX), and transmission electron microscopy (TEM). The procedures were carried out as previously described [29], with some changes. The functional groups on the surface of AgNPs, belonging to the compounds in bark extracts acting as capping/stabilizing agents, were detected by ATR-FTIR spectroscopy (Bruker Alpha-P ATR FTIR spectrometer, Bruker, Ettlingen, Germany). In brief, the aqueous bark extracts (30 mL of each) were concentrated under reduced pressure at 40 °C (Büchi R-210 rotary evaporator system, Büchi Labortechnik AG, Flawil, Switzerland) and freeze-dried (Unicryo TFD 5505 freeze dryer, UniEquip GmbH, Munich, Germany). Freeze-dried extracts and AgNPs pellets were subjected to ATR-FTIR spectroscopy in the spectral region of 4000–400 cm^{-1} with a resolution of 4 cm^{-1}. The size and morphology of AgNPs

were investigated by SEM coupled with EDX and TEM. For SEM-EDX measurements, a Quanta 200 scanning electron microscope equipped with an energy dispersive spectrometer (FEI Company, Hillsboro, OR, USA) was used. AgNPs pellets were analyzed in low vacuum mode at an operating voltage of 10 kV. TEM analyses, operated at 100 keV, were performed using a Hitachi High-Tech HT7700 transmission electron microscope (Hitachi High-Technologies Corporation, Tokyo, Japan) equipped with a Bruker EDX detector. Prior to analysis, colloidal AgNPs solutions (a drop of each) were placed on carbon-coated copper grids (300-mesh) and subjected to 24 h vacuum-drying (room temperature). DLS measurements were made on a Malvern Zetasizer Nano-ZS (Malvern Instruments, Malvern, UK). The hydrodynamic diameters and polydispersity index (PDI) values of the colloidal AgNPs solutions were determined using He/Ne laser (λ = 633 nm); electrophoretic light scattering was used to measure zeta potential. The colloidal AgNPs solutions refer to the reaction mixtures in which the synthesis of AgNPs was completed (before separation of AgNPs by centrifugation).

2.9. Assessment of Antioxidant Activity

2.9.1. DPPH Radical Scavenging Assay

The antioxidant potential of synthesized AgNPs was initially evaluated by the DPPH radical scavenging assay [37]. A volume of 1800 μL of 0.002% DPPH solution in methanol was mixed with 200 μL of various dilutions of AgNPs in ultra-pure water (50–500 μg/mL). After 30 min incubation at room temperature in dark, the absorbance was determined at 515 nm (Specord 210 Plus spectrophotometer, Analytik Jena, Jena, Thuringia, Germany). Trolox (50–500 μg/mL) was used as positive control. The DPPH radical scavenging activity (%) was calculated as follows: $100 \times (A_C - A_S)/A_C$, where A_C and A_S are the absorbances of the control (DPPH solution) and sample (AgNPs, Trolox), respectively. The experiments were carried out in triplicate.

2.9.2. ABTS Radical Cation Scavenging Assay

The ABTS radical cation was generated by incubating ABTS (7 mM) with potassium persulfate (2.54 mM) for 16 h in dark at room temperature; the solution was further diluted with ethanol to an absorbance of 0.70 $\pm$ 0.02 at 734 nm (Specord 210 Plus spectrophotometer, Analytik Jena, Jena, Thuringia, Germany). In brief, the ABTS radical cation solution (1500 μL) was mixed with different concentrations (50–500 μg/mL) of AgNPs/Trolox (positive control). The absorbance was recorded at 734 nm after 6 min incubation at room temperature [31,38]. ABTS radical cation scavenging activity was calculated as described in Section 2.9.1. The assay was performed in triplicate.

2.10. Assessment of Cell Toxicity

2.10.1. Cell Cultures

Vero and A-375 cells were cultured in DMEM supplemented with 2% (Vero cells) and 10% (A-375 cells) fetal bovine serum and antibiotics (100 μg/mL penicillin, 100 IU/mL streptomycin) and placed in an incubator at 37 °C in humidified atmosphere (5% CO_2, 95% air) until an optimal cell confluence (at least 90%) was reached [39].

2.10.2. Assessment of Cell Viability

A. alba and *P. sylvestris* bark extract-derived AgNPs were applied at different concentrations ranging from 3.125 to 25 μg/mL, for 24 and 48 h. Cell viability was evaluated using the MTT assay as previously reported [40,41], with minor changes. Briefly, the cells were detached with trypsin/EDTA, counted, resuspended in 96-well microplates (7×10^3 cells/well), and maintained in the conditions mentioned above (Section 2.10.1). Once the monolayer formed (24 h), the cells were treated with *A. alba* or *P. sylvestris* bark extract-derived AgNPs. After 24/48 h treatment, the medium was removed, and the cells were washed with phosphate-buffered saline, followed by the addition of fresh growth medium (100 μL/well) and MTT (5 mg/mL, 10 μL/well) and incubation for 3 h at 37 °C

(5% CO_2, 95% air). DMSO (100 µL/well) was further added to solve the insoluble formazan crystals generated after MTT reduction [42–44]. The absorbance of the formazan dye was quantified at 570 nm using a microplate reader (Biochrom, Berlin, Germany). The cell viability (%) was calculated as follows: $A_S/A_C \times 100$, where A_S and A_C are the absorbances of the formazan dye produced in samples (treated cells) and control (untreated cells), respectively. The experiments were performed in triplicate.

2.10.3. Assessment of Cell Morphology

Morphological changes in Vero and A-375 cells after 24 and 48 h treatment were examined using a Nikon Eclipse TS100 inverted microscope (Nikon, Tokyo, Japan) equipped with a digital camera (MSHOT MS60).

2.11. Assessment of Antibacterial Activity

The antibacterial activity of AgNPs was evaluated using the broth microdilution method as previously described [45,46], with slight modifications. Prior to the experiment, stock solutions of AgNPs and ciprofloxacin were prepared (*A. alba* and *P. sylvestris* bark extract-derived AgNPs: 250 µg/mL, ciprofloxacin: 2560 µg/mL) and further subjected to two-fold serial dilutions. AgNPs and ciprofloxacin stock solutions and dilutions were prepared in sterile ultra-pure water. In brief, 30 µL of 0.5 McFarland standard bacterial inoculum was mixed with two-fold serial dilutions of AgNPs (30 µL) or antibiotic (10 µL) and Mueller-Hinton broth up to 200 µL; the mixtures were incubated for 24 h at 37 °C followed by an evaluation of bacterial growth. The minimum inhibitory concentration (MIC) value was the lowest concentration of an antibacterial agent that completely inhibited the growth of bacteria [46,47].

2.12. Data Analysis

The total phenolic content was expressed as mean ± standard deviation (SD). The antioxidant activity was expressed as EC_{50} values (half maximal effective concentration) calculated by linear interpolation between the values above and below 50% activity; the results were expressed as mean ± SD. The cytotoxic activity was expressed as IC_{50} values (concentration of sample producing 50% inhibition of cell viability) using the polynomial graphic plots by modeling the percentage of cytotoxicity vs. concentration of AgNPs; the results were expressed as mean ± standard error (SE). The paired *t*-test was used to assess the differences between samples and control.

3. Results

### 3.1. Chemical Characterization of Bark Extracts

The results are presented in the Supplementary File (Supplementary Figure S1, Supplementary Table S1).

3.2. Optimization of Synthesis Parameters

For the synthesis of AgNPs, *A. alba/P. sylvestris* bark aqueous extract was mixed with $AgNO_3$ under continuous stirring. Different parameters (pH, $AgNO_3$ concentration, ratio between the volume of bark extract and $AgNO_3$, temperature, and reaction time) were optimized for the synthesis of AgNPs which was monitored by UV-Vis spectroscopy (Figure 1). The generation of AgNPs was indicated by a color change and a characteristic absorption band (Surface Plasmon Resonance (SPR) band) in the visible domain (400–500 nm), caused by the collective oscillations of the free electrons at the surface of metallic Ag when excited by light [48].

To evaluate the effect of pH on AgNPs synthesis, the process was conducted at various pH values (2, 4, 6, 8, and 10). For both bark extracts, the synthesis of AgNPs could not be achieved at acidic pH (pH 2). At pH 4 and 6, slightly prominent bands between 400 and 500 nm indicated that the synthesis of AgNPs was initiated. At basic pH (8 and 10), characteristic SPR peaks were observed in the region of 410–430 nm, supporting the

formation of AgNPs. In the case of both bark extracts, at pH 10, SPR peaks were sharper and their absorption maxima slightly shifted to shorter wavelengths (Figure 1A,B) suggesting the formation of smaller-sized AgNPs [49]. A single sharp SPR band at short wavelengths indicates the synthesis of small and spherical AgNPs while broader SPR bands (two or three) at longer wavelengths are characteristic of anisotropic and large AgNPs [50,51]. So, pH 10 was chosen for the synthesis of *A. alba* and *P. sylvestris* bark extract-derived AgNPs.
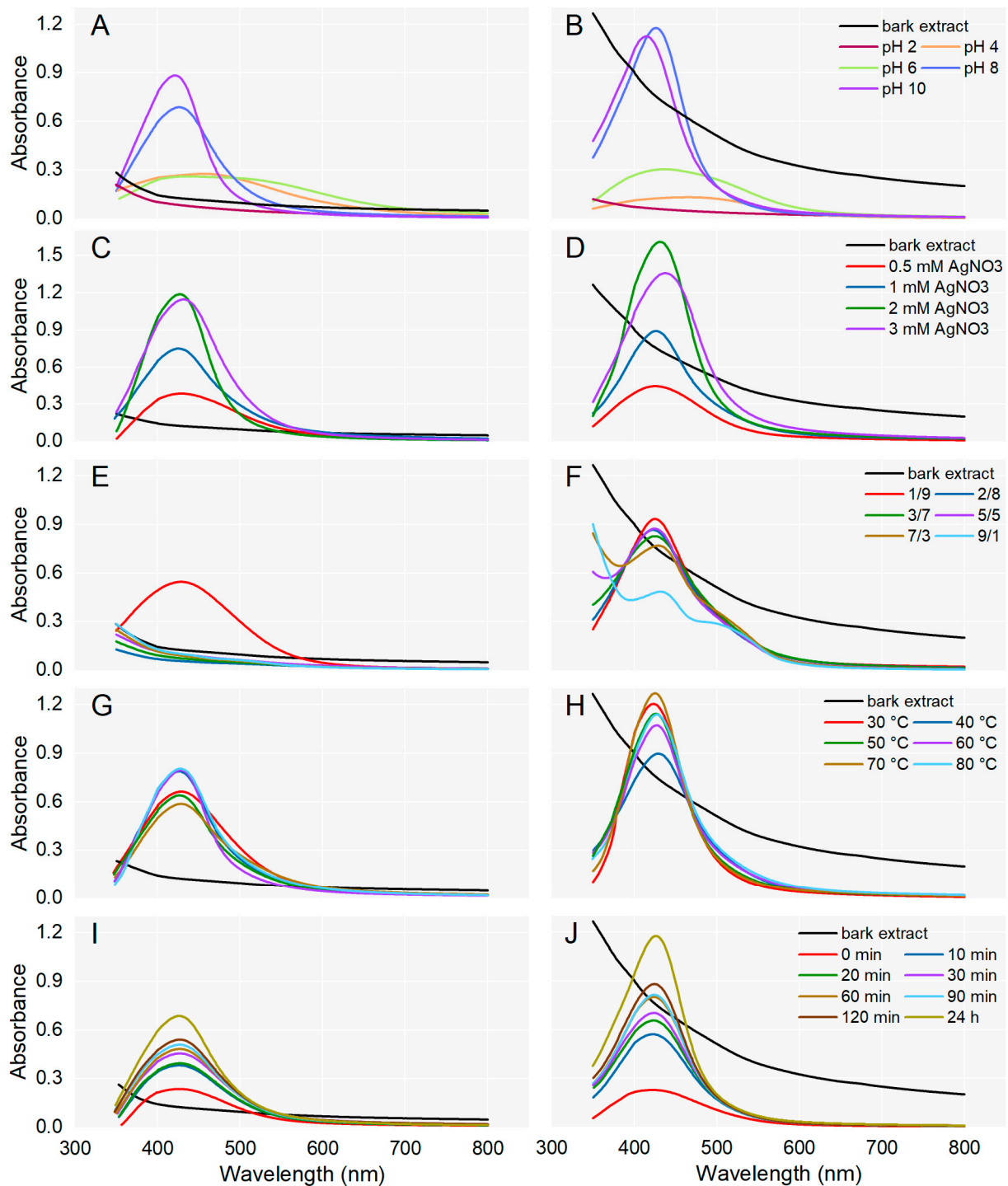
Figure 1. Effect of pH, AgNO$_3$ concentration, ratio between the volumes of plant extract and AgNO$_3$, temperature, and reaction time on the synthesis of AgNPs from *Abies alba* (**A,C,E,G,I**) and *Pinus sylvestris* (**B,D,F,H,J**) bark aqueous extracts.

The concentration of AgNO$_3$ solution is another parameter that significantly affected the synthesis of AgNPs. As shown in Figure 1C,D, for both *A. alba* and *P. sylvestris* bark extract-derived AgNPs, the absorption increased up to 2 mM AgNO$_3$. At 3 mM AgNO$_3$, the absorbance started to decrease and the SPR bands became broader and slightly shifted to longer wavelengths. It seems that higher AgNO$_3$ concentrations impair the synthesis and moreover, lead to larger AgNPs. The best SPR peak (as intensity, shape, and position) was obtained at 2 mM AgNO$_3$, and therefore this concentration was chosen as the optimal one for the synthesis of AgNPs.

The effect of the volume ratio of bark extract to 2 mM AgNO$_3$ on AgNPs synthesis was investigated in several proportions (1:9, 2:8, 3:7, 5:5, 7:3, and 9:1). In the case of *A. alba* bark extract, AgNPs were synthesized only when the bark extract and AgNO$_3$ were used at a ratio of 1:9 (*v/v*); no AgNPs synthesis was observed at other ratios used in the experiment (Figure 1E). For *P. sylvestris* bark extract-derived AgNPs, the highest SPR band was achieved at a similar ratio of bark extract to 2 mM AgNO$_3$ (1:9, *v/v*); the intensity of the SPR band decreased as the volume of bark extract increased (Figure 1F). Hence, a bark extract to AgNO$_3$ (2 mM) ratio of 1:9 (*v/v*) was chosen as optimal for the synthesis of AgNPs.

The effect of temperature on AgNPs synthesis was evaluated using temperature values ranging from 30 to 80 °C and previously optimized parameters. In the case of *A. alba* bark extract-derived AgNPs, sharp peaks appeared when the synthesis was conducted at 40, 60, and 80 °C (absorption maximum at 426, 428, and 427 nm, respectively). Smaller and broader peaks were generated at 30, 50, and 70 °C (Figure 1G). For *P. sylvestris* bark extract-derived AgNPs, the best yields were obtained at 30 and 70 °C. At 30 °C, the absorption maximum was observed at 423 nm; at 70 °C, it shifted to 425 nm (Figure 1H). The temperature values of 60, 80, and 70 °C shifted the absorption maximum of *A. alba* and *P. sylvestris* bark extract-derived AgNPs, respectively, to longer wavelengths, indicating that AgNPs size increased. Therefore, 40 and 30 °C were chosen as optimal temperatures for the synthesis of AgNPs from *A. alba* and *P. sylvestris* bark extract, respectively.

To evaluate the effect of reaction time on AgNPs synthesis, *A. alba*/*P. sylvestris* bark aqueous extract was mixed with 2 mM AgNO$_3$ (1:9, *v/v*, pH of reaction mixture adjusted to 10 with 0.1 N NaOH) and stirred at 40 °C/30 °C for 120 min. AgNPs synthesis was checked at different time intervals (0–120 min) during stirring and at 24 h after the end of stirring. As shown in Figure 1I,J, for both bark extracts, the reduction of Ag$^+$ started immediately after the addition of the reducing agent (bark extract) to the AgNO$_3$ solution (0 min). At each time interval, an absorbance peak at around 420 nm indicated the synthesis of AgNPs. The yield of AgNPs increased as the reaction time increased. Therefore, a period of 120 min stirring followed by 24 h at rest was considered optimal for the synthesis of AgNPs.

The optimized experimental parameters for the synthesis of AgNPs were pH 10, the temperature of 30 and 40 °C (for *P. sylvestris* and *A. alba* bark extract-derived AgNPs, respectively), 2 mM AgNO$_3$, bark extract to AgNO$_3$ (2 mM) ratio of 1:9 (*v/v*), and 120 min reaction time (followed by 24 h at rest).

3.3. Characterization of AgNPs

A. alba and *P. sylvestris* bark extract-derived AgNPs, synthesized under optimized conditions, were characterized by ATR-FTIR spectroscopy, DLS, TEM, and SEM with EDX analyses.

ATR-FTIR spectroscopy was used to identify the functional groups of the compounds in bark extracts involved in the synthesis and stabilization of AgNPs. As shown in Figure 2, *A. alba* and *P. sylvestris* bark extracts exhibited broad bands at 3259 and 3269 cm^{-1}, respectively, corresponding to the stretching vibrations of the hydroxyl groups of polyphenols and polysaccharides [52]. Bands at 2925 and 2929 cm^{-1} (*A. alba* and *P. sylvestris* bark extract, respectively) belong to the stretching vibrations of the methylene groups [53]. Bands around 1600 and 1500 cm^{-1} (both bark extracts), 1443 cm^{-1} (*A. alba* bark extract), and 1262 cm^{-1} (*P. sylvestris* bark extract) could be ascribed to the stretching vibrations of the aromatic rings and =C–O–C groups of flavonoids [29,54]. The bands around 1600 and 1500 cm^{-1} could

also belong to the amide region in proteins [29,53,55]. The bands at 1027 and 1025 cm^{-1} (*A. alba* and *P. sylvestris* bark extract, respectively) are characteristic of the C–O–C stretching vibrations in carbohydrates [29,56,57]. The aromatic C–H out-of-plane bending vibrations are indicated by the bands at 816 cm^{-1} (both bark extracts) and 775 cm^{-1} (*P. sylvestris* bark extract), the latter suggesting the presence of flavonoids (B ring) [29,58]. ATR-FTIR spectra of AgNPs illustrate shifts in the bark extract bands confirming the involvement of some phytochemicals (polyphenols, carbohydrates, proteins) in the formation of AgNPs (reduction of Ag$^+$ to metallic Ag), but also in their stabilization. The bands at 3259 and 3269 cm^{-1} in *A. alba* and *P. sylvestris* bark extracts, respectively, not only shifted, but they attenuated and broadened, indicating the participation of polyphenols/polysaccharides in the synthesis of AgNPs.
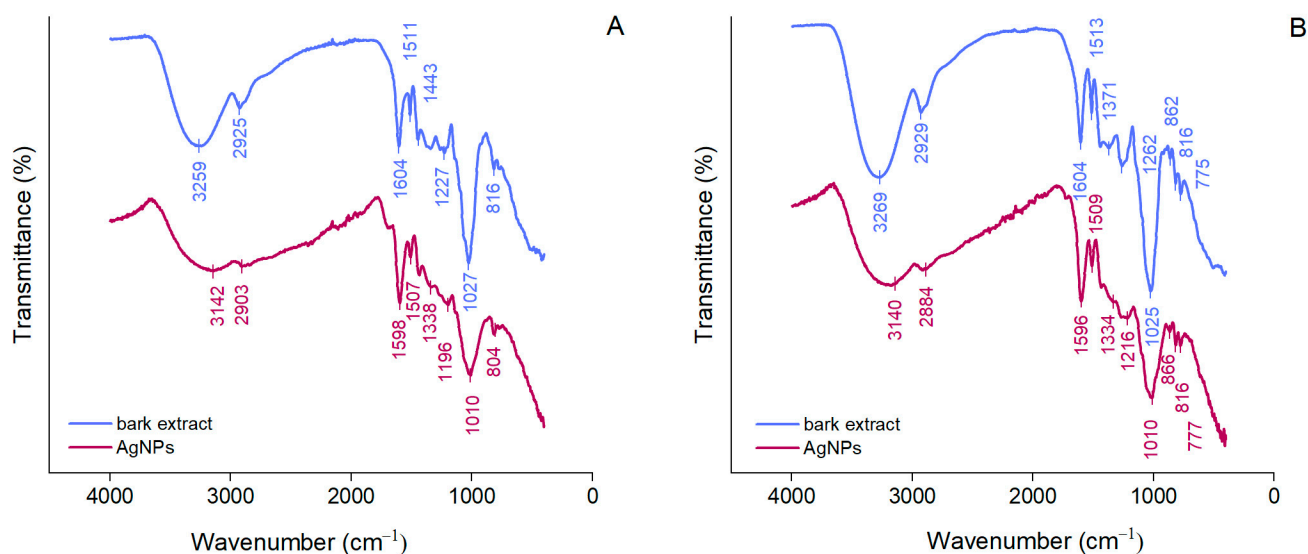
Figure 2. ATR-FTIR spectra of *Abies alba* (**A**) and *Pinus sylvestris* (**B**) bark aqueous extracts and their derived AgNPs.

Polyphenols majorly contributed to the synthesis and stabilization of AgNPs. Their contribution is also supported by a significant decrease in the phenolic contents of the reaction mixtures after the synthesis and separation of AgNPs (supernatants) (*A. alba*: 152.01 ± 11.16 µg/mL in the reaction mixture vs. 18.88 ± 3.09 µg/mL in supernatant; *P. sylvestris*: 608.15 ± 9.33 µg/mL in the reaction mixture vs. 432.71 ± 3.89 µg/mL in the supernatant).

DLS analysis was performed to determine the mean hydrodynamic diameter (Z-average), PDI, and zeta potential values for estimating the size of AgNPs in colloidal suspension, their dispersion, and stability, respectively [59]. *A. alba* bark extract-derived AgNPs showed a Z-average value of 62.84 nm and 2 peak values in the hydrodynamic diameter distribution (25.84 and 190.3 nm) (Figure 3A). For *P. sylvestris* bark extract-derived AgNPs, a single peak (106.5 nm) with a narrow base was obtained, indicating better homogeneity; the average particle size (Z-average) was 84.35 nm (Figure 3B). PDI value is an indicator of the homogeneity of the size distribution of AgNPs in colloidal dispersion. Low PDI values (below 0.7) reflect a narrow range of particle sizes and high uniformity [60]. In this study, PDI values indicated that *P. sylvestris* bark extract-derived AgNPs had a narrower distribution and better homogeneity in comparison with those derived from *A. alba* bark extract (0.221 vs. 0.334) (Figure 3A,B). The zeta potential indicates the charge on the surface of AgNPs and predicts their stability in colloidal dispersion, with values of ±10–20 mV reflecting a relatively stable colloid system [55,61]. Both *A. alba* and *P. sylvestris* bark extract-derived AgNPs showed similar negative values for zeta potential (−10.9 and −10.8 mV, respectively) (Figure 3A,B).
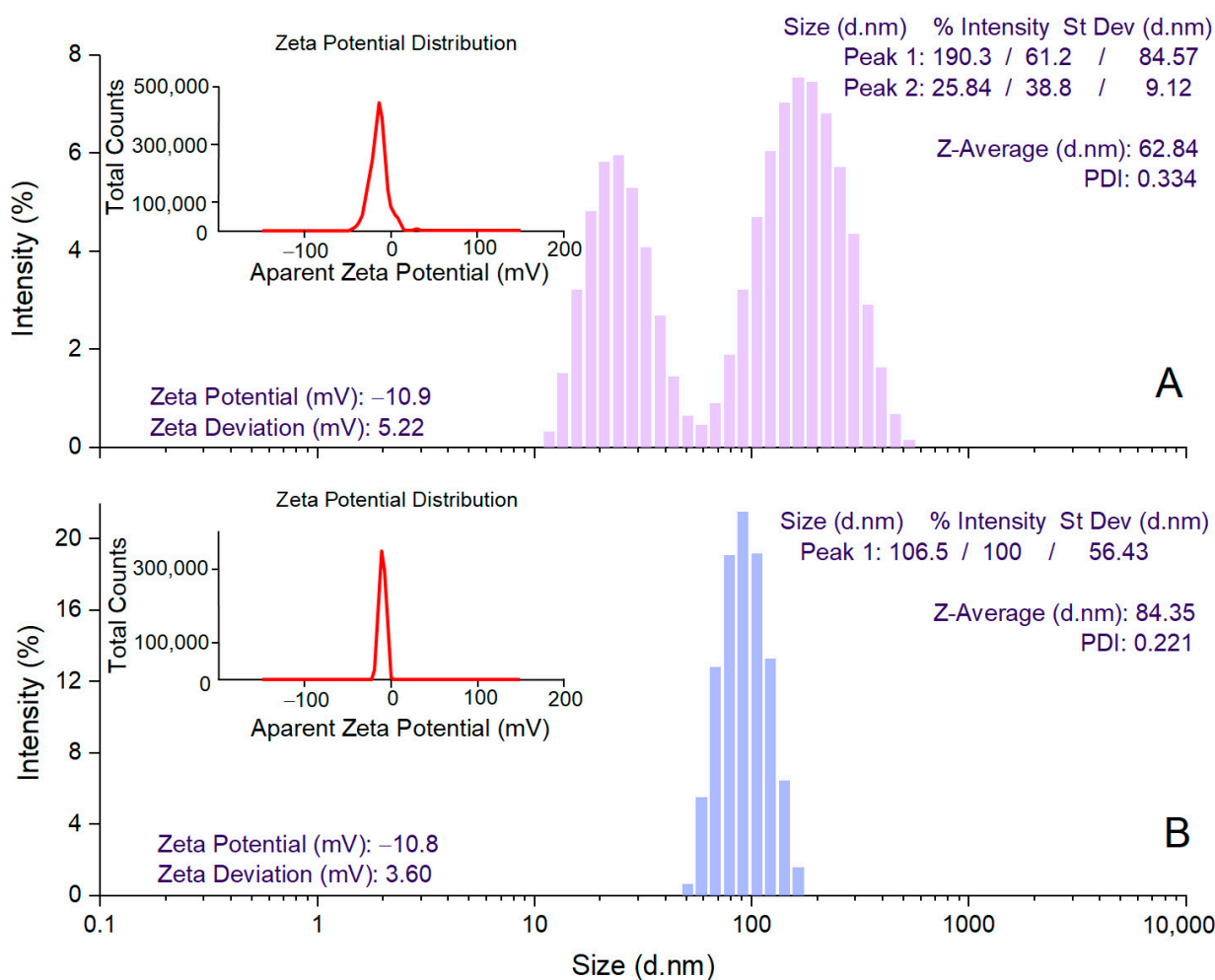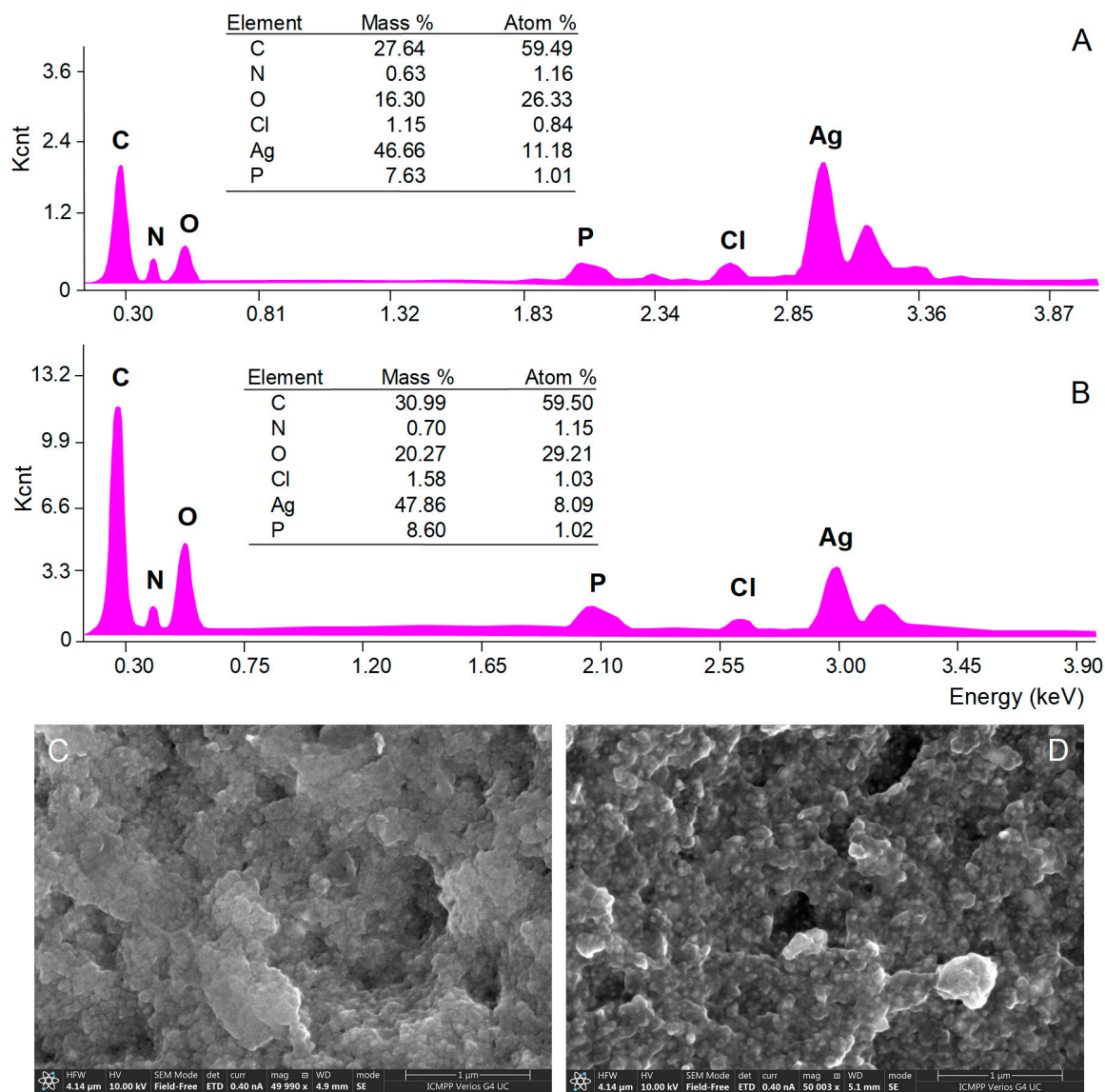
Figure 3. DLS analysis of *Abies alba* (**A**) and *Pinus sylvestris* (**B**) bark extract-derived AgNPs.

The morphology of AgNPs' surface and their elemental composition were investigated by SEM with EDX analyses. SEM micrograph images showed aggregations of spherical nanoparticles (Figure 4C,D), most probably caused by the procedures used to isolate AgNPs from the reaction mixtures (centrifugation followed by freeze-frying). EDX analysis provides qualitative and quantitative information on the chemical composition of AgNPs [34]. The EDX spectra of both *A. alba* and *P. sylvestris* bark extract-derived AgNPs (Figure 4A,B, respectively) revealed a pronounced signal for metallic Ag at 3 keV which confirmed the formation of AgNPs. Several other signals were registered for C, N, O, P, and Cl belonging to the compounds in bark extracts acting as capping agents [33,62].

The spherical shape of *A. alba* and *P. sylvestris* bark extract-derived AgNPs was confirmed by TEM (Figure 5A,B,D,E). In contrast to SEM micrographs, TEM images showed that the synthesized AgNPs were well-dispersed. This disparity might have its origin in sample preparation for analysis. As already mentioned, AgNPs as pellets, obtained by centrifugation and freeze-drying, were analyzed by SEM, whereas AgNPs as colloidal dispersion were subjected to TEM. Centrifugation followed by freeze-frying promoted AgNPs agglomeration, which was visible in SEM micrographs. Colloidal AgNPs formed in situ had a good dispersion rate, as illustrated by TEM analysis. Both *A. alba* and *P. sylvestris* bark extract-derived AgNPs showed lighter margins attributed to the compounds in bark extracts which adhered to the surface of AgNPs, thus capping and stabilizing them [63,64]. The presence of metallic Ag was revealed by TEM-EDX mapping (Figure 5C,F) confirming the reduction of Ag^+ to Ag^0 by the compounds present in bark extracts. *A. alba* bark extract-derived AgNPs ranged from 6 to 13 nm, whereas *P. sylvestris* bark extract-derived

AgNPs were larger (12–31 nm). By fitting the histogram data with a Gaussian distribution, the average particle size was found to be 9.92 and 24.49 nm for *A. alba* and *P. sylvestris* bark extract-derived AgNPs, respectively (Figure 5G,H).


Element	Mass %	Atom %
C	27.64	59.49
N	0.63	1.16
O	16.30	26.33
Cl	1.15	0.84
Ag	46.66	11.18
P	7.63	1.01

Element	Mass %	Atom %
C	30.99	59.50
N	0.70	1.15
O	20.27	29.21
Cl	1.58	1.03
Ag	47.86	8.09
P	8.60	1.02

Figure 4. Elemental composition (EDX spectra) and SEM micrographs of *Abies alba* (**A,C**) and *Pinus sylvestris* (**B,D**) bark extract-derived AgNPs.

3.4. Antioxidant Activity

Both *A. alba* and *P. sylvestris* bark extract-derived AgNPs scavenged the DPPH radical in a dose-dependent manner. For *A. alba* bark extract-derived AgNPs, the scavenging activity increased from $19.65 \pm 1.24\%$ (at 50 µg/mL) to $77.13 \pm 0.40\%$ (at 500 µg/mL). In the same concentration range, the scavenging ability of *P. sylvestris* bark extract-derived AgNPs varied from $21.42 \pm 0.53\%$ to $69.00 \pm 1.20\%$. At 50 µg/mL, Trolox, the positive control, showed $45.62 \pm 0.56\%$ scavenging activity, whereas at 150 µg/mL, it almost completely scavenged the DPPH radical ($97.20 \pm 0.94\%$) (Figure 6A). For EC_{50} calculation, additional dilutions of Trolox up to 10 µg/mL ($13.48 \pm 0.65\%$ DPPH scavenging activity) were tested. According to the EC_{50} values, *P. sylvestris* bark extract-derived AgNPs were slightly more active than *A. alba* bark extract-derived AgNPs; Trolox was approximately six times more active than bark extract-derived AgNPs (Table 1).
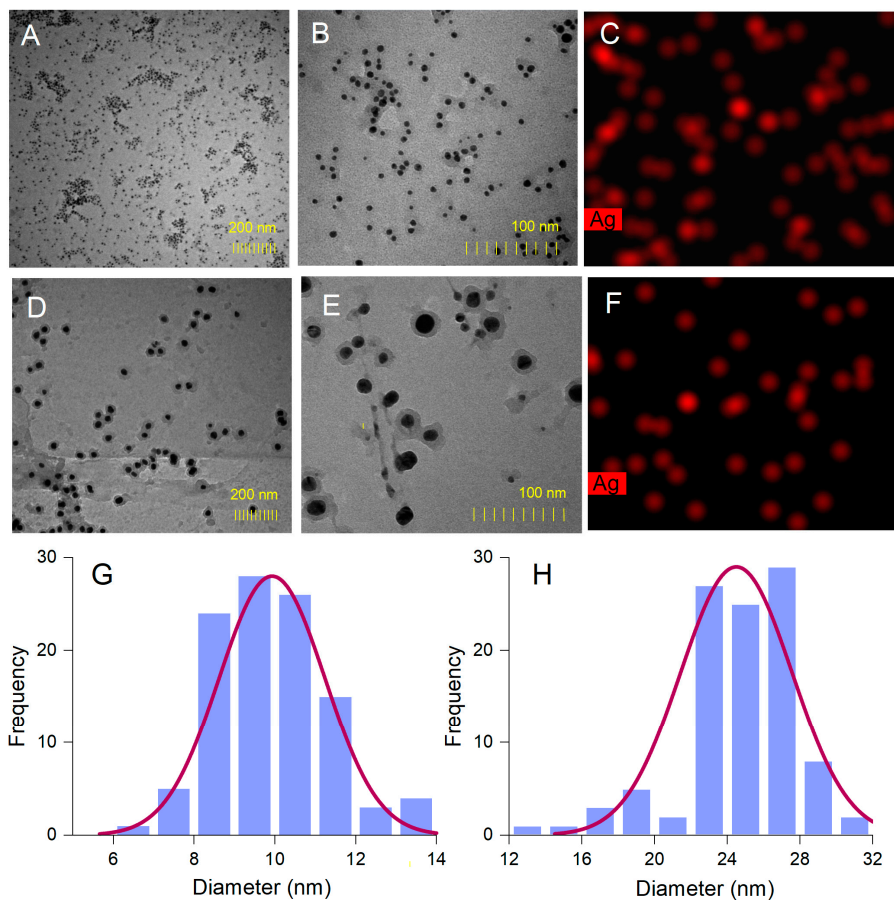
Figure 5. *Abies alba* bark extract-derived AgNPs: TEM images (**A**,**B**), TEM-EDX mapping (**C**), size-distribution histogram (**G**); *Pinus sylvestris* bark extract-derived AgNPs: TEM images (**D**,**E**), TEM-EDX mapping (**F**), and size-distribution histogram (**H**).
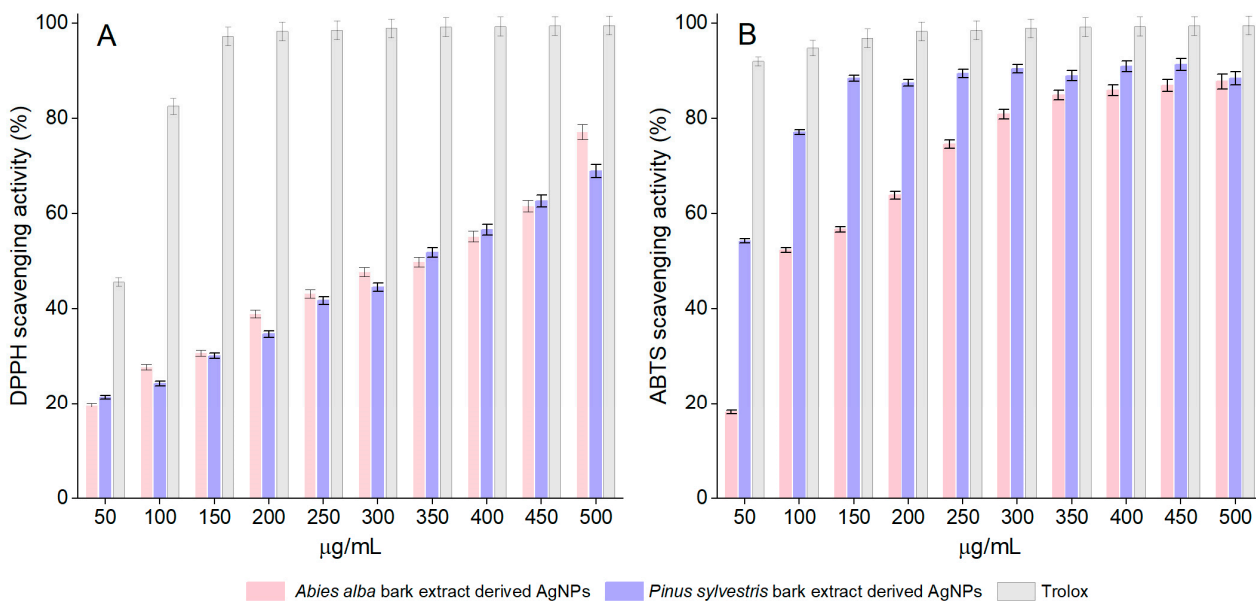
Figure 6. DPPH scavenging activity (**A**) and ABTS scavenging activity (**B**) of *Abies alba* and *Pinus sylvestris* bark extract-derived AgNPs and Trolox; significant differences ($p < 0.001$) between *Abies alba*/*Pinus sylvestris* bark extract-derived AgNPs and Trolox (at all tested concentrations).

Table 1. Antioxidant and cytotoxic activity of *Abies alba* and *Pinus sylvestris* bark extract-derived AgNPs.

Sample	EC_{50} (µg/mL)		IC_{50} (µg/mL) *	
	Antioxidant Activity		**Cytotoxicity (MTT Assay)**	
	DPPH Assay	**ABTS Assay**	**A-375 Cells**	**Vero Cells**
A. alba bark extract-derived AgNPs	351.7 ± 3.5	98.6 ± 0.3	2.40 ± 0.21	2.76 ± 0.39
P. sylvestris bark extract-derived AgNPs	336.7 ± 3.7	37.8 ± 0.4	6.02 ± 0.61	9.71 ± 0.87
Trolox	56.2 ± 0.8	11.4 ± 0.1	ND	ND

ND, not determined; * after 48 h treatment.

The synthesized AgNPs dose-dependently scavenged the ABTS radical cation. The scavenging activity of *A. alba* and *P. sylvestris* bark extract-derived AgNPs increased from $18.15 \pm 0.36\%$ and $54.26 \pm 1.08\%$, respectively (at 50 µg/mL) to $87.76 \pm 1.75\%$ and $88.45 \pm 1.76\%$, respectively (at 500 µg/mL). At 50 µg/mL, Trolox showed $91.98 \pm 1.83\%$ scavenging activity, whereas at 150 µg/mL, its scavenging activity increased to $99.50 \pm 1.99\%$ (Figure 6B). The ABTS radical cation scavenging activity varied as follows: Trolox > *P. sylvestris* bark extract-derived AgNPs > *A. alba* bark extract-derived AgNPs (Table 1).

3.5. Cytotoxic Activity

A. alba and *P. sylvestris* bark extract-derived AgNPs negatively impacted cell viability in a time- and dose-dependent manner. After 48 h treatment, the viability of A-375 cells exposed to *A. alba* bark extract-derived AgNPs (12.5 µg/mL) significantly decreased to $22.32 \pm 3.48\%$. At higher concentrations (25 µg/mL), a slight increase in cell viability ($26.12 \pm 0.57\%$) was noticed (Figure 7A). A similar tendency was observed in Vero cells, namely $37.11 \pm 1.84\%$ and $40.90 \pm 2.65\%$ viability in cells treated with 12.5 and 25 µg/mL *A. alba* bark extract-derived AgNPs, respectively (Figure 7B). When A-375 and Vero cells were exposed to *P. sylvestris* bark extract-derived AgNPs (12.5 and 25 µg/mL) for 48 h, the following cell viability percentages were detected: $27.02 \pm 0.36\%$, $24.10 \pm 0.72\%$, and $42.46 \pm 1.20\%$, $38.95 \pm 3.15\%$, respectively (Figure 7C,D). According to the IC_{50} values (after 48 h treatment), *A. alba* bark extract-derived AgNPs were more cytotoxic to A-375 cells; both bark extract-derived AgNPs were less cytotoxic to Vero cells (Table 1).
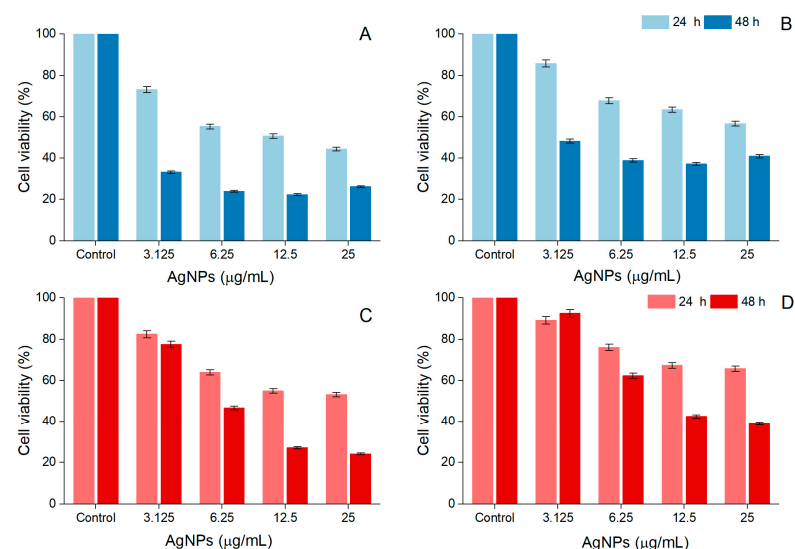
Figure 7. Viability of A-375 human malignant melanoma cells exposed to *Abies alba* (**A**) and *Pinus sylvestris* bark extract-derived AgNPs (**C**); viability of African green monkey kidney (Vero) cells exposed to *Abies alba* (**B**) and *Pinus sylvestris* bark extract-derived AgNPs (**D**); significant differences ($p < 0.001$) between *Abies alba*/*Pinus sylvestris* bark extract-derived AgNPs (at all tested concentrations) and control.

The microscopic investigation revealed a decrease in cell density and substrate adhesion capacity together with membrane shrinkage after exposure to *A. alba* and *P. sylvestris* bark extract-derived AgNPs, the processes being more intense after 48 h exposure. In contrast, the control cells showed a high confluence of the monolayer, intact cell membrane, and smooth morphology (without roughness) (Figure 8).
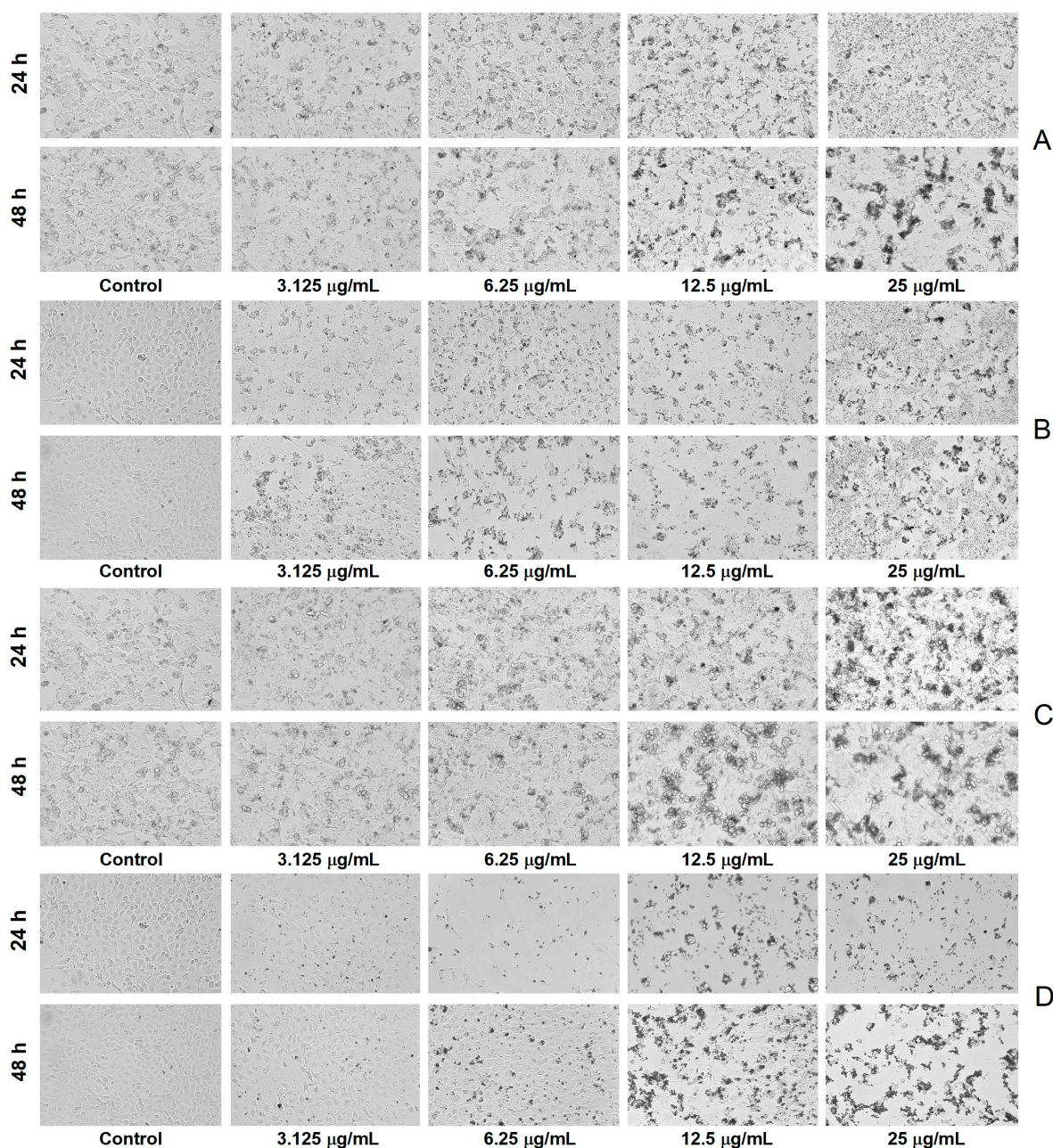
Figure 8. Bright-field morphological aspects of cells exposed to *Abies alba* bark extract-derived AgNPs ((**A**)—A-375 human malignant melanoma cells, (**B**)—African green monkey kidney (Vero) cells) and *Pinus sylvestris* bark extract-derived AgNPs ((**C**)—A-375 human malignant melanoma cells, (**D**)—African green monkey kidney (Vero) cells); scale bar 100 µm (10× magnification).

3.6. Antibacterial Activity

The antibacterial activity of AgNPs was investigated against five pathogenic reference strains, including two resistant ones: methicillin-resistant *S. aureus* (MRSA) ATCC 43300 and *S. epidermidis* ATCC 12228. The former also showed resistance to oxacillin and gentamicin, whereas the latter proved to be resistant to tetracycline [65]. According to the MIC

values (Table 2), *A. alba* bark extract-derived AgNPs possessed good antibacterial activity, being more active than *P. sylvestris* bark extract-derived AgNPs against all tested bacteria except *P. aeruginosa* ATCC 9027. In addition, *A. alba* bark extract-derived AgNPs inhibited the growth of resistant bacteria (MRSA ATCC 43300, *S. epidermidis* ATCC 12228) while *P. sylvestris* bark extract-derived AgNPs showed no activity against these two strains in the tested concentration range (0.24–250 µg/mL).

Table 2. Antibacterial activity of *Abies alba* and *Pinus sylvestris* bark extract-derived AgNPs.

Sample	MIC (µg/mL)				
	S. aureus ATCC 25923	*S. aureus* ATCC 43300 (MRSA)	*S. epidermidis* ATCC 12228	*E. coli* ATCC 25922	*P. aeruginosa* ATCC 9027
A. alba bark extract-derived AgNPs	18.75	75.00	18.75	37.50	75.00
P. sylvestris bark extract-derived AgNPs	75.00	NA	NA	75.00	75.00
Ciprofloxacin	2.00	1.00	0.12	0.03	0.50

NA, no activity.

4. Discussion

The use of plant extracts for the preparation of AgNPs has important advantages over other methods (physical, chemical, mechanical, and microbial). Plant extract-mediated AgNPs synthesis is simple, fast, and cost-effective. Phytochemicals in plant extracts play a dual role, serving as both reducing agents and stabilizers of AgNPs. In addition, the method is eco-friendly as it produces less environmental contamination [8]. To date, different parts of coniferous trees (bark, stem, needles, cones, and even exudates such as gum) have been used for the synthesis of AgNPs with various biological effects (antimicrobial, anticancerous, antioxidant, and antipyretic) [19].

In our study, AgNPs were prepared using *A. alba* and *P. sylvestris* bark aqueous extracts. Both extracts were initially subjected to LC-HRMS/MS resulting in the identification/tentative identification of 22 compounds belonging to various phytochemical classes [25,30,66–75]. Of these compounds, several phenolics have already been reported in both conifer barks: catechin, gallocatechin, epicatechin, and lariciresinol in *A. alba* bark [23,76] and *O*-hexosides (*O*-glucosides) of hydroxybenzoic acid, vanillic acid, and taxifolin, procyanidin dimer, catechin, and taxifolin in *P. sylvestris* bark [21,25,27]. Apart from these phenolics, our study also spotted coumaroylquinic acids, terpenoid glycosides, and organic acids. Coumaroylquinic acids have been previously identified in the bark of other *Pinus* species such as *Pinus nigra* [29] and *Pinus densiflora* [77]. Mentha-2,8-dien-1-ol, menthane-3,8-diol, menth-2-en-1-ol, and cymen-8-ol are volatile monoterpenoids present in the essential oils isolated from various coniferous species [78–83]. On the basis of mass spectral data (Supplementary Table S1), previous investigations on MS/MS fragmentation of monoterpene glycosides [84,85], and the KNApSacK database [71], seven glycosides of the previously mentioned volatile monoterpenoids were tentatively identified in both bark extracts. Most fragment ions observed in the MS/MS spectra of these glycosides (compounds **9**, **18**, **22–26**) resulted from the loss of the hexosyl (162 Da), deoxyhexosyl (146 Da), and pentosyl (132 Da) residues, deprotonation, dehydration, and internal cleavage of sugar moieties. In addition, two dicarboxylic acids, azelaic (1,9-nonanedionic acid, compound **21**) and sebacic (1,10-decadienoic acid, compound **27**) acids, were tentatively identified. The former is an important signaling molecule in systemic acquired resistance, an inducible defense mechanism providing protection against pathogen infection [86]. Among the phytochemicals identified in bark extracts, polyphenols are highly involved in the synthesis and stabilization of AgNPs. The phenolic hydroxyl groups are responsible for the conversion of Ag^+ to Ag^0. At the same time, they cap around AgNPs, thus stabilizing them [3,8]. The involvement of polyphenols in the reduction of Ag^+ and stabilization of *A. alba* and *P. sylvestris* bark extract-derived AgNPs is supported by ATR-FTIR data and

also by a reduction of the total phenolic content in reaction mixtures after the synthesis and separation of AgNPs.

The biological effects of plant-derived AgNPs depend not only on the components of plant extracts but also on their physicochemical properties which are influenced by the synthesis parameters (pH, $AgNO_3$ concentration, ratio between the volumes of plant extract, $AgNO_3$, temperature, and reaction time) [3,12,33,35]. Therefore, in our study, we optimized the reaction conditions, taking into consideration the aforementioned parameters and monitoring the synthesis of AgNPs by UV-Vis spectroscopy. pH significantly affects the synthesis and stability of AgNPs. An alkaline pH facilitates the deprotonation of phenolic hydroxyl groups, thus enhancing their reduction abilities and consequently the synthesis of AgNPs [35]. At the same time, the amount of negative charge on the surface of AgNPs increases, the electrostatic repulsion between AgNPs becomes stronger, and their aggregation is lowered, resulting in small-sized, well-dispersed, and stable AgNPs. In addition, AgNPs synthesized in alkaline conditions have more regular shapes, usually spherical and hexagonal [87]. Basic pH values (8–12) were found to be optimal for the synthesis of AgNPs using extracts prepared from *Picea abies* bark [88,89], *Pinus eldarica* bark [90], *Pinus thunbergii* cones [91], *Bryophyllum pinnatum* leaves [33], *Oryza sativa* (Thai pigmented rice, riceberry) [35], *Syzygium jambos* leaves and bark [92], and *Givotia moluccana* leaves [53]. On the other hand, there are also studies reporting an optimal synthesis of AgNPs at neutral pH [51]. In our study, the synthesis of AgNPs was supported by an alkaline medium (pH 10). Another factor which dramatically affects the synthesis and stability of AgNPs is $AgNO_3$ concentration. Its increase results in higher yields of AgNPs but also a higher agglomeration rate. Moreover, an increase in $AgNO_3$ concentration above 10 mM causes the deposition of $AgNO_3$ on the surface of AgNPs, which may enhance their toxicity. Most studies showed that 1 mM $AgNO_3$ is the optimal concentration for AgNPs synthesis [51]. However, in some cases, small-sized AgNPs were synthesized using higher $AgNO_3$ concentrations. AgNPs of 15 and 20–50 nm were synthesized using 2 mM $AgNO_3$ and extracts obtained from *Crocus sativus* wastages [93] and *Chrysanthemum morifolium* flowers [94], respectively. AgNPs of 30–50 nm were obtained from *Chenopodium murale* leaf extract and 5 mM $AgNO_3$ [95]. The synthesis of monodispersed, spherical, and 9 nm sized AgNPs was achieved using *Hibiscus cannabinus* leaf extract and 5 mM $AgNO_3$ [96]. In our study, 9.92 and 24.49 nm sized AgNPs (according to TEM data) were produced from *A. alba* and *P. sylvestris* bark aqueous extracts, respectively, and 2 mM $AgNO_3$ in a ratio of 1:9 (*v/v*); an increase in the bark extract volume (ratios of 2:8, 3:7, 5:5, 7:3, and 9:1) impaired the synthesis of AgNPs. Other studies reported an optimal synthesis of AgNPs using *Picea abies* bark extract [89], *Aloe vera* leaf extract [97], *Rubus glaucus* fruit extract [98], *Thymus kotschyanus* plant extract [99], *Juglans regia* seed extract [100] or *Prunus serotina* cherry extract [101] and $AgNO_3$ (1 mM) in a ratio of 1:10 (*v/v*). An increase in $AgNO_3$ volume (*P. abies* bark extract and $AgNO_3$ in ratios of 1:50 and 1:100) significantly reduced the accumulation of AgNPs [89]. Temperature plays an important role in the synthesis of AgNPs. An increase in temperature enhances the kinetic energy of molecules and accelerates the reaction rate resulting in smaller-sized AgNPs and less AgNPs agglomeration [102]. On the other hand, high kinetic energy might enable multiple collisions and consequently, the aggregation and growth of AgNPs [103]. In our study, the optimal temperatures for the synthesis of *P. sylvestris* and *A. alba* bark extract-derived AgNPs were 30 and 40 °C, respectively. According to the literature data, a high-yield synthesis of uniformly sized, small, and spherical AgNPs was achieved at temperatures of 30–40 °C using leaf extracts of *Hibiscus cannabinus* [96], aloe [103], *Cynodon dactylon* [104], *Ocimum sanctum* [105], *Tephrosia purpurea* [106], *O. tenuiflorum, Solanum tricobatum, Syzygium cumini*, and *Centella asiatica* and peel extract of *Citrus sinensis* [107]. Reaction time affects both the yield and stability of AgNPs. Prolonged reaction times increase the yield of AgNPs but promote agglomeration of AgNPs, decreasing their stability [108]. There have been reported various reaction times in plant-mediated synthesis of AgNPs, e.g., 20 min [103], 30 min [35], 45 min [102], 1 h [104], 24–48 h [107], and 72 h [34]. In our study, a reaction

time of 120 min (followed by 24 h at rest) was found to be optimal for the synthesis of AgNPs using *A. alba* and *P. sylvestris* bark extracts.

The optimized parameters (pH 10, 30, and 40 °C for *P. sylvestris* and *A. alba* bark extract-derived AgNPs, respectively, 2 mM AgNO$_3$, bark extract to 2 mM AgNO$_3$ ratio of 1:9, *v/v*, and 120 min reaction time, followed by 24 h at rest) led to the synthesis of well-dispersed, spherical, small, and relatively stable AgNPs. Both DLS and TEM determined smaller average particle sizes for *A. alba* bark extract-derived AgNPs (62.84 and 9.92 nm, respectively, vs. 84.35 and 24.49 nm, respectively, for *P. sylvestris* bark extract-derived AgNPs). The difference in the average size between *A. alba* and *P. sylvestris* bark extract-derived AgNPs could be attributed to the different temperature values used in AgNPs synthesis (40 °C for *A. alba* bark extract-derived AgNPs, 30 °C for *P. sylvestris* bark extract-derived AgNPs) and AgNPs outer shell consisting of capping/stabilizing compounds. According to Verma and Mehata [102], as the temperature increases, the reaction rate quickens, resulting in smaller-sized AgNPs. In contrast to TEM, DLS analysis determined larger sizes (62.84 and 84.35 nm for *A. alba* and *P. sylvestris* bark extract-derived AgNPs, respectively). The discrepancy might be ascribed to the fact that DLS estimates the hydrodynamic diameter of AgNPs (the metallic core of AgNPs with the compounds adsorbed on their surface and the solvation shell), whereas TEM measures the geometric size of AgNPs [109]. The synthesized AgNPs were negatively charged (zeta potential values of −10.9 and −10.8 mV for *A. alba* and *P. sylvestris* bark extract-derived AgNPs, respectively). As already mentioned, polyphenols were involved in the synthesis and stabilization of AgNPs. According to Yang and Li (2013), an alkaline pH enhances the deprotonation of the phenolic hydroxyl groups of capping AgNPs, resulting in negatively charged hydroxylate ions on the surface of AgNPs [110]. The electrostatic repulsive forces between negatively charged AgNPs prevent their agglomeration, resulting in high dispersity and stability [55,111].

The synthesized AgNPs showed antioxidant, anticancer, and antibacterial effects. Both *A. alba* and *P. sylvestris* bark extract-derived AgNPs scavenged the DPPH radical (EC$_{50}$ = 351.70 and 336.70 μg/mL, respectively) and ABTS radical cation (EC$_{50}$ = 98.60 and 37.80 μg/mL, respectively), the scavenging activity being attributable to elemental Ag [112] but also to phytochemicals covering the surface of AgNPs [101,113]. The differences in antioxidant potency between *A. alba* and *P. sylvestris* bark extract-derived AgNPs are owing to the capping/stabilizing phytochemicals [38,101]. Our results are consistent with previous studies reporting DPPH [33,37,95,98,99,101,112,114] and ABTS [33,38,115–117] scavenging potential for AgNPs capped with plant constituents. In a similar DPPH experimental protocol, AgNPs synthesized using *Elephantopus scaber* leaf extract exhibited an IC$_{50}$ value of 126.6 μg/mL [37]. Other studies used various experimental protocols to evaluate the DPPH scavenging activity of the phytofunctionalized AgNPs. AgNPs synthesized using *Bryophyllum pinnatum* leaf extract scavenged the DPPH free radical with an IC$_{50}$ value of 89.05 μg/mL [33]. At 500 μg/mL, AgNPs prepared using *Iresine herbstii* leaf extract inactivated the radical by more than 70% [112]. At 100 μg/mL, the DPPH scavenging activity of AgNPs synthesized from *Rhododendron dauricum* flower extract was comparable to that of Trolox (approx. 70%) [114]. In various ABTS experimental protocols, AgNPs synthesized using extracts of *Hypericum perforatum* (aerial parts), *Origanum onites* (aerial parts), *Argyreia nervosa* (leaves), and *Bryophyllum pinnatum* (leaves) showed IC$_{50}$ values of 26.78 [38], 5.16 [115], 44.3 [116], and 259.14 μg/mL, respectively [33].

The anticancer potential of AgNPs has recently gained much attention. Various mechanisms are involved in the anticancer activity of AgNPs such as alteration of cell/lysosomal membrane integrity, increase in oxidative stress, induction of apoptosis, cell cycle arrest, and inhibition of angiogenesis [48,118]. The anticancer activity of AgNPs is considerably influenced by their size, shape, and zeta potential. A smaller size, an irregular shape, and a negative zeta potential are essential for good anticancer activity [119]. The use of plant extracts for the synthesis of AgNPs has produced phytofunctionalized AgNPs with remarkable anticancer properties. Plant extract-derived AgNPs proved to be active against different human cancer cell lines (lung, breast, liver, cervical, prostate, colon, ovarian,

etc.); some phytofunctionalized AgNPs displayed low IC_{50} values (<100 µg/mL) and/or showed less cytotoxicity against normal cells [8,120,121]. To the best of our knowledge, the cytotoxic potential of phytofunctionalized AgNPs against human melanoma cells has been scarcely investigated [122]. González-Pedroza et al. [123] have recently studied the cytotoxic effects of AgNPs synthesized using *Annona muricata* leaf and fruit peel aqueous extracts on A-375 human malignant melanoma cells and found a remarkable activity (IC_{50} = 2.004 and 1.285 µg/mL, respectively), with less toxicity to normal macrophages (IC_{50} = 10.7 and 13.7 µg/mL, respectively). *A. muricata* aqueous extracts contain polyphenols, acetogenins, and citric acid, which are responsible not only for the synthesis and stabilization of AgNPs but also for their anticancer activity. Acetogenins, for example, are well known for their pro-apoptotic effects [123]. Another study reported a significant reduction in the viability of A-375 cells after exposure to AgNPs obtained from the homeopathic mother tinctures (ethanolic extracts, 70% ethanol, *v/v*) of *Gelsemium sempervirens*, *Thuja occidentalis*, *Phytolacca decandra*, and *Hydrastis canadensis* (IC_{50} = 80, 120, 78, and 100 µg/mL, respectively). All AgNPs showed pro-apoptotic effects associated with DNA fragmentation, cell cycle arrest at the G2/M phase, and caspase-3 activation [119]. AgNPs synthesized using boswellic acid (isolated from the gum resin of *Boswellia serrata*) exerted cytotoxic activity on G361 human malignant melanoma cells, and the effect is comparable to that of doxorubicin [124]. In our study, *A. alba* and *P. sylvestris* bark extract-derived AgNPs showed significant cytotoxicity toward A-375 human malignant melanoma cells (IC_{50} = 2.40 and 6.02 µg/mL, respectively), being less cytotoxic against normal Vero cells (IC_{50} = 2.76 and 9.71 µg/mL, respectively) (after 48 h treatment). The smaller-sized *A. alba* bark extract-derived AgNPs exhibited higher cytotoxicity against both cell lines. Smaller AgNPs are more cytotoxic due to their more efficient interaction with cell membranes, resulting in a higher penetration rate and cellular uptake and consequently higher antitumor efficacy [3,13,121,125]. In addition, phytochemical capping AgNPs undoubtedly contribute to the anticancer activity of phytofunctionalized AgNPs. Our study showed that polyphenols in *A. alba* and *P. sylvestris* bark extracts are involved in the synthesis and stabilization of AgNPs. Among these polyphenols, catechins (catechin, epicatechin, gallocatechin, procyanidin oligomers) have been reported to inhibit melanoma cell growth and invasion by multiple mechanisms (cell cycle arrest, decrease in cyclooxygenase-2 expression, prostaglandin E_2 production, ERK1/2 phosphorylation, and NFκBp65 activation) [126]. Moreover, a pine bark extract—*Pinus maritima* (syn. *Pinus pinaster*), having 61.26 mg catechin/g, induced apoptosis in A-375 cells by increasing caspase-3 expression and activity. In addition, the extract reduced oxidative stress and down-regulated matrix metallopeptidase-9, an enzyme responsible for cell invasion and metastasis [127]. *A. alba* and *P. sylvestris* bark extract-derived AgNPs also altered cell morphology, most probably due to cytoskeleton damage [123].

AgNPs are well-known antimicrobial agents being active against Gram-positive and Gram-negative bacteria, fungi, and viruses, including drug-resistant strains. In brief, AgNPs adhere to the microbial cell surface through electrostatic forces disrupting the cell membrane integrity, penetrating inside the cell, and interacting with proteins, lipids, ribosomes, and DNA, causing severe cellular dysfunctions. AgNPs increase cellular oxidative stress and alter important signal transduction pathways (tyrosine phosphorylation) causing cell damage and death [4]. The antibacterial potential of AgNPs can be significantly improved by using plant extracts for their synthesis. Extracts from different parts of plants (leaves, flowers, fruits, seeds, peels, roots, rhizomes, bark, stem, and even gum, latex, and callus) and whole plants have been used for the synthesis of AgNPs with antibacterial effects. The capping phytochemicals but also the size of AgNPs significantly impact the antibacterial activity. A small size (<50 nm) provides a greater surface of interaction with the bacterial membrane, which enhances the antibacterial potency [12,128]. In our study, the stronger antibacterial activity of *A. alba* bark extract-derived AgNPs can be attributed, in large part, to their smaller size (9.92 vs. 24.49 nm for *P. sylvestris* bark extract-derived AgNPs). In addition, *A. alba* bark extract-derived AgNPs displayed the lowest MIC values

(18.75 µg/mL) against two Gram-positive bacteria (*S. aureus* ATCC 25923 and *S. epidermidis* ATCC 12228) which supports the contribution of capping phytochemicals to the antibacterial activity of AgNPs. As already mentioned, "naked" AgNPs are more effective against Gram-negative bacteria, whereas the phytofunctionalized ones have a broader antibacterial spectrum, including Gram-positive bacteria. Polyphenols, which cap and stabilize *A. alba* and *P. sylvestris* bark extract-derived AgNPs, have antimicrobial properties [31]. Catechins, for example, are more effective against Gram-positive bacteria. The antibacterial activity of catechins is associated with cytoplasmic membrane damage, alteration of membrane integrity, and cellular leakage. Catechins easily bind to the peptidoglycan layer of Gram-positive bacteria but hardly penetrate the lipopolysaccharide layers of Gram-negative bacteria [129]. AgNPs synthesized using plant extracts demonstrated efficacy against various bacteria, including those tested in the present study. *Eucalyptus globulus* leaf extract-derived AgNPs displayed antibacterial activity against MSSA, MRSA, and extended-spectrum β-lactamase *E. coli* and *P. aeruginosa* clinical isolates with MIC values of 30, 27, 36, and 27 µg/mL, respectively [130]. The MIC values of AgNPs prepared using *Musa paradisiaca* peel extract against MSSA (*S. aureus* ATCC 6538), *E. coli* ATCC 8739, and *P. aeruginosa* ATCC 9027 were 5.1, 3.4, and 1.7 µg/mL, respectively [34]. AgNPs obtained from *Alpinia katsumadai* seed extract inhibited the growth of *E. coli* (MIC = 20 µg/mL) and *P. aeruginosa* (MIC = 40 µg/mL) [131].

5. Conclusions

The results of the present study clearly demonstrate that *Abies alba* and *Pinus sylvestris* bark can be successfully used for the synthesis of bioactive AgNPs. *Abies alba* and *Pinus sylvestris* bark extract-derived AgNPs were well-dispersed, spherical, and small-sized (9.92 and 24.49 nm, respectively). The synthesized AgNPs had a pronounced cytotoxic activity against A-375 human malignant melanoma cells, being less cytotoxic to normal cells. They were also found to have antioxidant activity and antibacterial effects against Gram-positive and Gram-negative bacteria. *Abies alba* bark extract-derived AgNPs demonstrated stronger toxicity against A-375 human malignant melanoma cells as well as stronger antibacterial activity against *Staphylococcus aureus* (methicillin-sensitive and methicillin-resistant), *Staphylococcus epidermidis*, and *Escherichia coli*. The bioactivity of synthesized AgNPs was influenced by their size and capping/stabilizing phytochemicals on their surface. In conclusion, *Abies alba* and *Pinus sylvestris* bark extract-derived AgNPs exhibited antioxidant, antibacterial, and cytotoxic effects against A-375 human malignant melanoma cells. Further studies are needed for an in-depth assessment of their antioxidant, anticancer, and antimicrobial potential and also biocompatibility by using more normal tumor cell lines and bacterial strains.

Author Contributions: Conceptualization, I.M. and A.M.; methodology, I.M., S.V.L., K.S.-W., C.E.H., L.S., G.V., B.L.I. and A.C.; investigation, I.M., S.V.L., C.E.H., C.M.R., L.S., G.V., D.G., A.D.P. and C.N.; resources, C.N. and A.M.; writing—original draft preparation, I.M., S.V.L., C.E.H., C.M.R., G.V. and A.M.; writing—review and editing, K.S.-W., A.C. and A.M.; supervision, B.L.I., A.C. and A.M. All authors have read and agreed to the published version of the manuscript.

Institutional Review Board Statement: Not applicable.

Informed Consent Statement: Not applicable.

Data Availability Statement: The data presented in this study are available upon request from the corresponding author (Anca Miron, anca.miron@umfiasi.ro).

References

1. Keat, C.L.; Aziz, A.; Eid, A.M.; Elmarzugi, N.A. Biosynthesis of nanoparticles and silver nanoparticles. *Bioresour. Bioprocess.* **2015**, *2*, 1–11. [CrossRef]
2. Koduru, J.R.; Kailasa, S.K.; Bhamore, J.R.; Kim, K.-H.; Dutta, T.; Vellingiri, K. Phytochemical-assisted synthetic approaches for silver nanoparticles antimicrobial applications: A review. *Adv. Colloid Interface Sci.* **2018**, *256*, 326–339. [CrossRef]
3. Akintelu, S.A.; Bo, Y.; Folorunso, A.S. A review on synthesis, optimization, mechanism, characterization, and antibacterial application of silver nanoparticles synthesized from plants. *J. Chem.* **2020**, *2020*, 3189043. [CrossRef]
4. Dakal, T.C.; Kumar, A.; Majumdar, R.S.; Yadav, V. Mechanistic basis of antimicrobial actions of silver nanoparticles. *Front. Microbiol.* **2016**, *7*, 1831. [CrossRef] [PubMed]
5. Gurunathan, S.; Lee, K.J.; Kalishwaralal, K.; Sheikpranbabu, S.; Vaidyanathan, R.; Eom, S.H. Antiangiogenic properties of silver nanoparticles. *Biomaterials* **2009**, *30*, 6341–6350. [CrossRef] [PubMed]
6. Kovács, D.; Szőke, K.; Igaz, N.; Spengler, G.; Molnár, J.; Tóth, T.; Madarász, D.; Rázga, Z.; Kónya, Z.; Boros, I.M.; et al. Silver nanoparticles modulate ABC transporter activity and enhance chemotherapy in multidrug resistant cancer. *Nanomed. Nanotechnol. Biol. Med.* **2016**, *12*, 601–610. [CrossRef]
7. Benedec, D.; Oniga, I.; Cuibus, F.; Sevastre, B.; Stiufiuc, G.; Duma, M.; Hanganu, D.; Iacovita, C.; Stiufiuc, R.; Lucaciu, C.M. *Origanum vulgare* mediated green synthesis of biocompatible gold nanoparticles simultaneously possessing plasmonic, antioxidant and antimicrobial properties. *Int. J. Nanomed.* **2018**, *13*, 1041–1058. [CrossRef]
8. Rajan, R.; Chandran, K.; Harper, S.L.; Yun, S.I.; Kalaichelvan, P.T. Plant extract synthesized silver nanoparticles: An ongoing source of novel biocompatible materials. *Ind. Crops Prod.* **2015**, *70*, 356–373. [CrossRef]
9. Khanra, K.; Roy, A.; Bhattacharyya, N. Evaluation of antibacterial activity and cytotoxicity of green synthesized silver nanoparticles using *Hemidesmus Indicus* R. Br. *Am. J. Nanosci. Nanotechnol.* **2013**, *1*, 1–6.
10. Roy, A.; Khanra, K.; Mishra, A.; Bhattacharyya, N. Highly cytotoxic (PA-1), less cytotoxic (A549) and antimicrobial activity of a green synthesized silver nanoparticle using *Mikania cordata* L. *J. Adv. Res.* **2013**, *1*, 193–198.
11. Ramgopal, M.; Saisushma, C.H.; Alhasin, A.M. A facile green synthesis of silver nanoparticles using soap nuts. *Res. J. Microbiol.* **2011**, *6*, 432. [CrossRef]
12. Roy, A.; Bulut, O.; Some, S.; Mandal, A.K.; Yilmaz, M.D. Green synthesis of silver nanoparticles: Biomolecule-nanoparticle organizations targeting antimicrobial activity. *RSC Adv.* **2019**, *9*, 2673–2702. [CrossRef] [PubMed]
13. Jaffri, S.B.; Ahmad, K.S. Phytofunctionalized silver nanoparticles: Green biomaterial for biomedical and environmental applications. *Rev. Inorg. Chem.* **2018**, *38*, 127–149. [CrossRef]
14. Jini, D.; Sharmila, S. Green synthesis of silver nanoparticles from *Allium cepa* and its in vitro antidiabetic activity. *Mater. Today Proc.* **2020**, *22*, 432–438. [CrossRef]
15. Anbukkarasi, M.; Thomas, P.A.; Sheu, J.R.; Geraldine, P. In vitro antioxidant and anticataractogenic potential of silver nanoparticles biosynthesized using an ethanolic extract of *Tabernaemontana divaricata* leaves. *Biomed. Pharmacother.* **2017**, *91*, 467–475. [CrossRef]
16. Anbukkarasi, M.; Thomas, P.A.; Teresa, P.A.; Anand, T.; Geraldine, P. Comparison of the efficacy of a *Tabernaemontana divaricata* extract and of biosynthesized silver nanoparticles in preventing cataract formation in an *in-vivo* system of selenite-induced cataractogenesis. *Biocatal. Agric. Biotechnol.* **2020**, *23*, 101475. [CrossRef]
17. Ali, M.S.; Anuradha, V.; Yogananth, N.; Krishnakumar, S. Heart and liver regeneration in zebrafish using silver nanoparticle synthesized from *Turbinaria conoides–In vivo*. *Biocatal. Agric. Biotechnol.* **2019**, *17*, 104–109. [CrossRef]
18. Wang, Y.; Wei, S.; Wang, K.; Wang, Z.; Duan, J.; Cui, L.; Zheng, H.; Wang, Y.; Wang, S. Evaluation of biosynthesis parameters, stability and biological activities of silver nanoparticles synthesized by *Cornus Officinalis* extract under 365 nm UV radiation. *RSC Adv.* **2020**, *10*, 27173–27182. [CrossRef] [PubMed]
19. Bhardwaj, K.; Dhanjal, D.S.; Sharma, A.; Nepovimova, E.; Kalia, A.; Thakur, S.; Bhardwaj, S.; Chopra, C.; Singh, R.; Verma, R.; et al. Conifer-derived metallic nanoparticles: Green synthesis and biological applications. *Int. J. Mol. Sci.* **2020**, *21*, 9028. [CrossRef]
20. Bhardwaj, K.; Silva, A.S.; Atanassova, M.; Sharma, R.; Nepovimova, E.; Musilek, K.; Sharma, R.; Alghuthaymi, M.A.; Dhanjal, D.S.; Nicoletti, M.; et al. Conifers phytochemicals: A valuable forest with therapeutic potential. *Molecules* **2021**, *26*, 3005. [CrossRef] [PubMed]
21. Amalinei, R.L.M.; Trifan, A.; Cioanca, O.; Miron, S.D.; Mihai, C.T.; Rotinberg, P.; Miron, A. Polyphenol-rich extract from *Pinus sylvestris* L. bark–chemical and antitumor studies. *Rev. Med. Soc. Med. Nat. Iaşi* **2014**, *118*, 551–557.
22. Vasincu, A.; Creţu, E.; Geangalău, I.; Mihăilescu Amalinei, R.L.; Miron, A. Polyphenolic content and antioxidant activity of an extractive fraction from *Abies alba* bark. *Rev. Med. Chir. Soc. Med. Nat. Iaşi* **2013**, *117*, 545–550.
23. Benković, E.T.; Grohar, T.; Žigon, D.; Švajger, U.; Janeš, D.; Kreft, S.; Štrukelj, B. Chemical composition of the silver fir (*Abies alba*) bark extract Abigenol® and its antioxidant activity. *Ind. Crops Prod.* **2014**, *52*, 23–28. [CrossRef]

24. Leone, K.; Micheletto, M.; Di Maira, G.; Tedesco, E.; Benetti, F.; Zaloker, U. Role of a novel silver fir (*Abies alba*) extract, Abigenol®/AlbiPhenol®, in modulating cardiovascular disorders: Key factors. *Antioxidants* **2022**, *11*, 618. [CrossRef]

25. Karonen, M.; Hämäläinen, M.; Nieminen, R.; Klika, K.D.; Loponen, J.; Ovcharenko, V.V.; Moilanen, E.; Pihlaja, K. Phenolic extractives from the bark of *Pinus sylvestris* L. and their effects on inflammatory mediators nitric oxide and prostaglandin E$_2$. *J. Agric. Food Chem.* **2004**, *52*, 7532–7540. [CrossRef]

26. Blomstrand, B.M.; Enemark, H.L.; Øines, Ø.; Steinshamn, H.; Aasen, I.M.; Mahnert, K.C.; Sørheim, K.M.; Athanasiadou, S.; Thamsborg, S.M.; Woolsey, I.D. Extracts of pine bark (*Pinus sylvestris*) inhibit *Cryptosporidium parvum* growth in cell culture. *Parasitol. Res.* **2021**, *120*, 2919–2927. [CrossRef] [PubMed]

27. Nisca, A.; Ștefănescu, R.; Stegăruș, D.I.; Mare, A.D.; Farczadi, L.; Tanase, C. Comparative Study Regarding the Chemical Composition and Biological Activity of Pine (*Pinus nigra* and *P. sylvestris*) Bark Extracts. *Antioxidants* **2021**, *10*, 327. [CrossRef]

28. Karthika, V.; Arumugam, A.; Gopinath, K.; Kaleeswarran, P.; Govindarajan, M.; Alharbi, N.S.; Kadaikunnan, S.; Khaled, J.M.; Benelli, G. *Guazuma ulmifolia* bark-synthesized Ag, Au and Ag/Au alloy nanoparticles: Photocatalytic potential, DNA/protein interactions, anticancer activity and toxicity against 14 species of microbial pathogens. *J. Photochem. Photobiol. B* **2017**, *167*, 189–199. [CrossRef] [PubMed]

29. Macovei, I.; Luca, S.V.; Skalicka-Woźniak, K.; Sacarescu, L.; Pascariu, P.; Ghilan, A.; Doroftei, F.; Ursu, E.L.; Rimbu, C.M.; Horhogea, C.E.; et al. Phyto-functionalized silver nanoparticles derived from conifer bark extracts and evaluation of their antimicrobial and cytogenotoxic effects. *Molecules* **2021**, *27*, 217. [CrossRef] [PubMed]

30. Luca, S.V.; Miron, A.; Aprotosoaie, A.C.; Mihai, C.-T.; Vochita, G.; Gherghel, D.; Ciocarlan, N.; Skalicka-Woźniak, K. HPLC-DAD-ESI-Q-TOF-MS/MS profiling of *Verbascum ovalifolium* Donn ex Sims and evaluation of its antioxidant and cytogenotoxic activities. *Phytochem. Anal.* **2019**, *30*, 34–45. [CrossRef] [PubMed]

31. Apetrei, C.L.; Tuchilus, C.; Aprotosoaie, A.C.; Oprea, A.; Malterud, K.E.; Miron, A. Chemical, antioxidant and antimicrobial investigations of *Pinus cembra* L. bark and needles. *Molecules* **2011**, *16*, 7773–7788. [CrossRef] [PubMed]

32. Singleton, V.L.; Rossi, J.A. Colorimetry of total phenolics with phosphomolybdic-phosphotungstic acid reagents. *Am. J. Enol. Vitic.* **1965**, *16*, 144–158.

33. Chandraker, S.K.; Lal, M.; Dhruve, P.; Singh, R.P.; Shukla, R. Cytotoxic, antimitotic, DNA binding, photocatalytic, H$_2$O$_2$ sensing, and antioxidant properties of biofabricated silver nanoparticles using leaf extract of *Bryophyllum pinnatum* (Lam.) Oken. *Front. Mol. Biosci.* **2021**, *7*, 465. [CrossRef] [PubMed]

34. Ibrahim, H.M. Green synthesis and characterization of silver nanoparticles using banana peel extract and their antimicrobial activity against representative microorganisms. *J. Radiat. Res. Appl. Sci.* **2015**, *8*, 265–275. [CrossRef]

35. Jiamboonsri, P.; Wanwong, S. Photoassisted synthesis of silver nanoparticles using riceberry rice extract and their antibacterial application. *J. Nanomater.* **2021**, *2021*, 5598924. [CrossRef]

36. Sarsar, V.; Selwal, M.K.; Selwal, K.K. Biogenic synthesis, optimisation and antibacterial efficacy of extracellular silver nanoparticles using novel fungal isolate *Aspergillus fumigatus* MA. *IET Nanobiotechnol.* **2016**, *10*, 215–221. [CrossRef]

37. Kharat, S.N.; Mendhulkar, V.D. Synthesis, characterization and studies on antioxidant activity of silver nanoparticles using *Elephantopus scaber* leaf extract. *Mater. Sci. Eng. C* **2016**, *62*, 719–724. [CrossRef]

38. Alahmad, A.; Feldhoff, A.; Bigall, N.C.; Rusch, P.; Scheper, T.; Walter, J.G. *Hypericum perforatum* L.-mediated green synthesis of silver nanoparticles exhibiting antioxidant and anticancer activities. *Nanomaterials* **2021**, *11*, 487. [CrossRef]

39. Vunjak-Novakovic, G. Basic principles of Cell Culture. In *Culture of Cells for Tissue Engineering*; Vunjak-Novakovic, G., Freshney, R.I., Eds.; John Wiley & Sons: Hoboken, NJ, USA, 2006; Volume 7, pp. 1–22.

40. Laville, N.; Aït-Åssa, S.; Gomez, E.; Casellas, C.; Porcher, J.M. Effects of human pharmaceuticals on cytotoxicity, EROD activity and ROS production in fish hepatocytes. *Toxicology* **2004**, *196*, 41–55. [CrossRef]

41. Mosmann, T. Rapid colorimetric assay for cellular growth and survival: Application to proliferation and cytotoxicity assays. *J. Immunol. Meth.* **1983**, *65*, 55–63. [CrossRef]

42. Berridge, M.V.; Herst, P.M.; Tan, A.S. Tetrazolium dyes as tools in cell biology: New insights into their cellular reduction. *Biotechnol. Annu. Rev.* **2005**, *11*, 127–152. [CrossRef]

43. Stockert, J.C.; Blázquez-Castro, A.; Cañete, M.; Horobin, R.W.; Villanueva, Á. MTT assay for cell viability: Intracellular localization of the formazan product is in lipid droplets. *Acta Histochem.* **2012**, *114*, 785–796. [CrossRef] [PubMed]

44. Van Meerloo, J.; Kaspers, G.J.L.; Cloos, J. Cell sensitivity assays: The MTT assay. *Methods Mol. Biol.* **2011**, *731*, 237–245. [CrossRef] [PubMed]

45. Aelenei, P.; Rimbu, C.M.; Horhogea, C.E.; Lobiuc, A.; Neagu, A.N.; Dunca, S.I.; Motrescu, I.; Dimitriu, G.; Aprotosoaie, A.C.; Miron, A. Prenylated phenolics as promising candidates for combination antibacterial therapy: Morusin and kuwanon G. *Saudi Pharm. J.* **2020**, *28*, 1172–1181. [CrossRef] [PubMed]

46. Massadeh, M.I.; Al-Masri, M.O.N.A.; Lf, A.Q. Antibacterial activity of *Peganum harmala* extracts and their green silver nanoparticles against acne associated bacteria. *Farmacia* **2022**, *70*, 5. [CrossRef]

47. Vega-Jimenez, A.L.; Vazquez-Olmos, A.R.; Acosta-Gio, E.; Alvarez-Perez, M.A. In vitro antimicrobial activity evaluation of metal oxide nanoparticles. In *Nanoemulsions: Properties, Fabrication and Application*; Koh, K.S., Wong, V.L., Eds.; IntechOpen: Rijecka, Croatia, 2019. [CrossRef]

48. Jain, N.; Jain, P.; Rajput, D.; Patil, U.K. Green synthesized plant-based silver nanoparticles: Therapeutic prospective for anticancer and antiviral activity. *Micro Nano Lett.* **2021**, *9*, 5. [CrossRef]

49. Soris, P.T.; Beulah, G.G.P.; Doss, A.; Mohan, V.R. *Croton sparsiflorus* whole plant extract mediated biosynthesis of metallic silver nanoparticles and their antibacterial activity. *J. Drug Deliv. Ther.* **2018**, *8*, 91–97. [CrossRef]

50. Kumar, R.; Roopan, S.M.; Prabhakarn, A.; Khanna, V.G.; Chakroborty, S. Agricultural waste *Annona squamosa* peel extract: Biosynthesis of silver nanoparticles. *Spectrochim. Acta Part A Mol. Biomol. Spectrosc.* **2012**, *90*, 173–176. [CrossRef]

51. Mashwani, Z.U.R.; Khan, T.; Khan, M.A.; Nadhman, A. Synthesis in plants and plant extracts of silver nanoparticles with potent antimicrobial properties: Current status and future prospects. *Appl. Microbiol. Biotechnol.* **2015**, *99*, 9923–9934. [CrossRef] [PubMed]

52. Kumari, R.; Saini, A.K.; Kumar, A.; Saini, R.V. Apoptosis induction in lung and prostate cancer cells through silver nanoparticles synthesized from *Pinus roxburghii* bioactive fraction. *J. Biol. Inorg. Chem.* **2020**, *25*, 23–37. [CrossRef]

53. Sana, S.S.; Dogiparthi, L.K. Green synthesis of silver nanoparticles using *Givotia moluccana* leaf extract and evaluation of their antimicrobial activity. *Mater. Lett.* **2018**, *226*, 47–51. [CrossRef]

54. Adib, A.M.; Jamaludin, F.; Kiong, L.S.; Hashim, N.; Abdullah, Z. Two-dimensional correlation infrared spectroscopy applied to analyzing and identifying the extracts of *Baeckea frutescens* medicinal materials. *J. Pharm. Biomed. Anal.* **2014**, *96*, 104–110. [CrossRef]

55. Patra, S.; Mukherjee, S.; Barui, A.K.; Ganguly, A.; Sreedhar, B.; Patra, C.R. Green synthesis, characterization of gold and silver nanoparticles and their potential application for cancer therapeutics. *Mater. Sci. Eng. C* **2015**, *53*, 298–309. [CrossRef]

56. Harshiny, M.; Matheswaran, M.; Arthanareeswaran, G.; Kumaran, S.; Rajasree, S. Enhancement of antibacterial properties of silver nanoparticles–ceftriaxone conjugate through *Mukia maderaspatana* leaf extract mediated synthesis. *Ecotoxicol. Environ. Saf.* **2015**, *121*, 135–141. [CrossRef] [PubMed]

57. Katas, H.; Lim, C.S.; Azlan, A.Y.H.N.; Buang, F.; Busra, M.F.M. Antibacterial activity of biosynthesized gold nanoparticles using biomolecules from *Lignosus rhinocerotis* and chitosan. *Saudi Pharm. J.* **2019**, *27*, 283–292. [CrossRef]

58. Konai, N.; Raidandi, D.; Pizzi, A.; Meva'a, L. Characterization of *Ficus sycomorus* tannin using ATR-FT MIR, MALDI-TOF MS and 13C NMR methods. *Eur. J. Wood Wood Prod.* **2017**, *75*, 807–815. [CrossRef]

59. Jebril, S.; Jenana, R.K.B.; Dridi, C. Green synthesis of silver nanoparticles using *Melia azedarach* leaf extract and their antifungal activities: In vitro and in vivo. *Mater. Chem. Phys.* **2020**, *248*, 122898. [CrossRef]

60. Nasiriboroumand, M.; Montazer, M.; Barani, H. Preparation and characterization of biocompatible silver nanoparticles using pomegranate peel extract. *J. Photochem. Photobiol. B Biol.* **2018**, *179*, 98–104. [CrossRef]

61. Bhattacharjee, S. DLS and zeta potential–what they are and what they are not? *J. Control Release* **2016**, *235*, 337–351. [CrossRef] [PubMed]

62. Ahmad, N.; Sharma, S. Green synthesis of silver nanoparticles using extracts of *Ananas comosus*. *Green Sustain. Chem.* **2012**, *2*, 24781. [CrossRef]

63. Jagtap, U.B.; Bapat, V.A. Green synthesis of silver nanoparticles using *Artocarpus heterophyllus* Lam. seed extract and its antibacterial activity. *Ind. Crop Prod.* **2013**, *46*, 132–137. [CrossRef]

64. Tripathi, D.; Modi, A.; Narayan, G.; Rai, S.P. Green and cost effective synthesis of silver nanoparticles from endangered medicinal plant *Withania coagulans* and their potential biomedical properties. *Mater. Sci. Eng. C* **2019**, *100*, 152–164. [CrossRef]

65. Aelenei, P.; Rimbu, C.M.; Guguianu, E.; Dimitriu, G.; Aprotosoaie, A.C.; Brebu, M.; Horhogea, C.E.; Miron, A. Coriander essential oil and linalool–interactions with antibiotics against Gram-positive and Gram-negative bacteria. *Lett. Appl. Microbiol.* **2019**, *68*, 156–164. [CrossRef] [PubMed]

66. Bujor, A.; Miron, A.; Luca, S.V.; Skalicka-Woźniak, K.; Silion, M.; Trifan, A.; Girard, C.; Demougeot, C.; Totoson, P. Vasorelaxant effects of *Crataegus pentagyna*: Links with arginase inhibition and phenolic profile. *J. Ethnopharmacol.* **2020**, *252*, 112559. [CrossRef] [PubMed]

67. Bujor, A.; Miron, A.; Luca, S.V.; Skalicka-Woźniak, K.; Silion, M.; Ancuceanu, R.; Dinu, M.; Girard, C.; Demougeot, C.; Totoson, P. Metabolite profiling, arginase inhibition and vasorelaxant activity of *Cornus mas*, *Sorbus aucuparia* and *Viburnum opulus* fruit extracts. *Food Chem. Toxicol.* **2019**, *133*, 110764. [CrossRef] [PubMed]

68. Cretu, E.; Karonen, M.; Salminen, J.-P.; Mircea, C.; Trifan, A.; Charalambous, C.; Constantinou, A.I.; Miron, A. *In vitro* study on the antioxidant activity of a polyphenol-rich extract from *Pinus brutia* bark and its fractions. *J. Med. Food* **2013**, *16*, 984–991. [CrossRef]

69. Karar, M.G.E.; Kuhnert, N. UPLC-ESI-Q-TOF-MS/MS characterization of phenolics from *Crataegus monogyna* and *Crataegus laevigata* (Hawthorn) leaves, fruits and their herbal derived drops (Crataegutt Tropfen). *J. Chem. Biol. Ther.* **2015**, *1*, 102. [CrossRef]

70. Yuzuak, S.; Ballington, J.; Xie, D.Y. HPLC-qTOF-MS/MS-based profiling of flavan-3-ols and dimeric proanthocyanidins in berries of two muscadine grape hybrids FLH 13-11 and FLH 17-66. *Metabolites* **2018**, *8*, 57. [CrossRef]

71. 'KNApSAcK' Family. Available online: http://www.knapsackfamily.com/KNApSAcK_Family/ (accessed on 21 December 2022).

72. Yang, C.-J.; Wang, Z.-B.; Mi, Y.-Y.; Gao, M.-J.; Lv, J.-N.; Meng, Y.-H.; Yang, B.-Y.; Kuang, H.-X. UHPLC-MS/MS determination, pharmacokinetic, and bioavailability study of taxifolin in rat plasma after oral administration of its nanodispersion. *Molecules* **2016**, *21*, 494. [CrossRef]

73. Saber, F.R.; Mohsen, E.; El-Hawary, S.; Eltanany, B.M.; Elimam, H.; Sobeh, M.; Elmotayam, A.K. Chemometric-enhanced metabolic profiling of five *Pinus* species using HPLC-MS/MS spectrometry: Correlation to in vitro anti-aging, anti-Alzheimer and antidiabetic activities. *J. Chromatogr. B* **2021**, *1177*, 122759. [CrossRef]

74. Zhang, X.; Liang, C.; Li, C.; Bu, M.; Bu, L.; Xiao, Y.; Sun, H.; Zhang, L. Simultaneous qualitative and quantitative study of main compounds in *Commelina communis* Linn. by UHPLC–Q-TOF-MS-MS and HPLC–ESI-MS-MS. *J. Chromatogr. Sci.* **2018**, *56*, 582–594. [CrossRef]

75. Rizzarelli, P.; Zampino, D.; Ferreri, L.; Impallomeni, G. Direct electrospray ionization mass spectrometry quantitative analysis of sebacic and terephthalic acids in biodegradable polymers. *Anal. Chem.* **2011**, *83*, 654–660. [CrossRef] [PubMed]

76. Brennan, M.; Fritsch, C.; Cosgun, S.; Dumarcay, S.; Colin, F.; Gerardin, P. Quantitative and qualitative composition of bark polyphenols changes longitudinally with bark maturity in *Abies alba* Mill. *Ann. For. Sci.* **2020**, *77*, 1–14. [CrossRef]

77. Kim, K.J.; Hwang, E.S.; Kim, M.J.; Rha, C.S.; Song, M.C.; Maeng, S.; Park, J.H.; Kim, D.O. Effects of Phenolic-Rich *Pinus densiflora* Extract on Learning, Memory, and Hippocampal Long-Term Potentiation in Scopolamine-Induced Amnesic Rats. *Antioxidants* **2022**, *11*, 2497. [CrossRef] [PubMed]

78. Ankney, E.; Swor, K.; Satyal, P.; Setzer, W.N. Essential Oil Compositions of *Pinus* Species (*P. contorta* Subsp. *contorta*, *P. ponderosa* var. *ponderosa*, and *P. flexilis*); Enantiomeric Distribution of Terpenoids in *Pinus* Species. *Molecules* **2022**, *27*, 5658. [CrossRef] [PubMed]

79. Halloum, B.; Shakya, A.K.; Elagbar, Z.A.; Naik, R.R. GC-MS Analysis and Biological activity of Essential Oil of Fruits, Needles and Bark of *Pinus pinea* grown wildly in Jordan. *Acta Pol. Pharm.* **2019**, *76*, 825–831. [CrossRef]

80. Lee, J.H.; Yang, H.Y.; Lee, H.S.; Hong, S.K. Chemical composition and antimicrobial activity of essential oil from cones of *Pinus koraiensis*. *J. Microbiol. Biotechnol.* **2008**, *18*, 497–502.

81. Lis, A.; Swaczyna, A.; Krajewska, A.; Mellor, K. Chemical composition of the essential oils from twigs, leaves, and cones of *Thuja plicata* and its cultivar varieties "fastigiata", "kornik," and "zebrina". *Nat. Prod. Commun.* **2019**, *14*, 1934578X19862904. [CrossRef]

82. Mitić, Z.S.; Jovanović, S.Č.; Zlatković, B.K.; Nikolić, B.M.; Stojanović, G.S.; Marin, P.D. Needle terpenes as chemotaxonomic markers in *Pinus*: Subsections *Pinus* and *Pinaster*. *Chem. Biodivers.* **2017**, *14*, e1600453. [CrossRef]

83. Özgenç, Ö.; Durmaz, S.; Çelik, G.; Korkmaz, B.; Yaylı, N. Comparative phytochemical analysis of volatile organic compounds by SPME-GC-FID/MS from six coniferous and nine deciduous tree bark species grown in Turkey. *S. Afr. J. Bot.* **2017**, *113*, 23–28. [CrossRef]

84. Flamini, R.; De Rosso, M.; Panighel, A.; Dalla Vedova, A.; De Marchi, F.; Bavaresco, L. Profiling of grape monoterpene glycosides (aroma precursors) by ultra-high performance-liquid chromatography-high resolution mass spectrometry (UHPLC/QTOF). *J. Mass Spectrom.* **2014**, *49*, 1214–1222. [CrossRef]

85. Wei, Y.; Chen, Z.; Zhang, X.K.; Duan, C.Q.; Pan, Q.H. Comparative analysis of glycosidic aroma compound profiling in three *Vitis vinifera* varieties by using ultra-high-performance liquid chromatography quadrupole-time-of-flight mass spectrometry. *Front. Plant Sci.* **2021**, *12*, 1271. [CrossRef]

86. Ádám, A.L.; Nagy, Z.Á.; Kátay, G.; Mergenthaler, E.; Viczián, O. Signals of systemic immunity in plants: Progress and open questions. *Int. J. Mol. Sci.* **2018**, *19*, 1146. [CrossRef] [PubMed]

87. Handayani, W.; Ningrum, A.S.; Imawan, C. The role of pH in synthesis silver nanoparticles using *Pometia pinnata* (matoa) leaves extract as bioreductor. *J. Phys. Conf. Ser.* **2020**, *1428*, 012021. [CrossRef]

88. Tanase, C.; Berta, L.; Coman, N.A.; Roșca, I.; Man, A.; Toma, F.; Mocan, A.; Nicolescu, A.; Jakab-Farkas, L.; Biró, D.; et al. Antibacterial and antioxidant potential of silver nanoparticles biosynthesized using the spruce bark extract. *Nanomaterials* **2019**, *9*, 1541. [CrossRef]

89. Tanase, C.; Berta, L.; Mare, A.; Man, A.; Talmaciu, A.I.; Roșca, I.; Mircia, E.; Volf, I.; Popa, V.I. Biosynthesis of silver nanoparticles using aqueous bark extract of *Picea abies* L. and their antibacterial activity. *Eur. J. Wood Wood Prod.* **2020**, *78*, 281–291. [CrossRef]

90. Iravani, S.; Zolfaghari, B. Green synthesis of silver nanoparticles using *Pinus eldarica* bark. *Biomed. Res. Int.* **2013**, *2013*, 1–5. [CrossRef]

91. Velmurugan, P.; Lee, S.M.; Iydroose, M.; Lee, K.J.; Oh, B.T. Pine cone-mediated green synthesis of silver nanoparticles and their antibacterial activity against agricultural pathogens. *Appl. Microbiol. Biotechnol.* **2013**, *97*, 361–368. [CrossRef] [PubMed]

92. Dutta, P.P.; Bordoloi, M.; Gogoi, K.; Roy, S.; Narzary, B.; Bhattacharyya, D.R.; Mohapatra, P.K.; Mazumder, B. Antimalarial silver and gold nanoparticles: Green synthesis, characterization and in vitro study. *Biomed. Pharmacother.* **2017**, *91*, 567–580. [CrossRef] [PubMed]

93. Bagherzade, G.; Tavakoli, M.M.; Namaei, M.H. Green synthesis of silver nanoparticles using aqueous extract of saffron (*Crocus sativus* L.) wastages and its antibacterial activity against six bacteria. *Asian Pac. J. Trop. Biomed.* **2017**, *7*, 227–233. [CrossRef]

94. He, Y.; Du, Z.; Lv, H.; Jia, Q.; Tang, Z.; Zheng, X.; Zhang, K.; Zhao, F. Green synthesis of silver nanoparticles by *Chrysanthemum morifolium* Ramat. extract and their application in clinical ultrasound gel. *Int. J. Nanomed.* **2013**, *8*, 1809. [CrossRef] [PubMed]

95. Abdel-Aziz, M.S.; Shaheen, M.S.; El-Nekeety, A.A.; Abdel-Wahhab, M.A. Antioxidant and antibacterial activity of silver nanoparticles biosynthesized using *Chenopodium murale* leaf extract. *J. Saudi Chem. Soc.* **2014**, *18*, 356–363. [CrossRef]

96. Bindhu, M.R.; Umadevi, M. Synthesis of monodispersed silver nanoparticles using *Hibiscus cannabinus* leaf extract and its antimicrobial activity. *Spectrochim. Acta A Mol. Biomol. Spectrosc.* **2013**, *101*, 184–190. [CrossRef] [PubMed]

97. Yadav, J.P.; Kumar, S.; Budhwar, L.; Yadav, A.; Yadav, M. Characterization and antibacterial activity of synthesized silver and iron nanoparticles using *Aloe vera*. *J. Nanomed. Nanotechnol.* **2016**, *384*, 2. [CrossRef]

98. Kumar, B.; Smita, K.; Cumbal, L.; Debut, A. Green synthesis of silver nanoparticles using Andean blackberry fruit extract. *Saudi J. Biol. Sci.* **2017**, *24*, 45–50. [CrossRef]

99. Hamelian, M.; Zangeneh, M.M.; Amisama, A.; Varmira, K.; Veisi, H. Green synthesis of silver nanoparticles using *Thymus kotschyanus* extract and evaluation of their antioxidant, antibacterial and cytotoxic effects. *Appl. Organomet. Chem.* **2018**, *32*, 4458. [CrossRef]

100. Mehnath, S.; Sathishkumar, G.; Arivoli, A.; Rajan, M.; Praphakar, R.A.; Jeyaraj, M. Green synthesis of AgNPs by Walnut seed extract and its role in photocatalytic degradation of a textile dye effluent. *Trans. Eng. Sci.* **2017**, *5*, 31–40.

101. Kumar, B.; Angulo, Y.; Smita, K.; Cumbal, L.; Debut, A. Capuli cherry-mediated green synthesis of silver nanoparticles under white solar and blue LED light. *Particuology* **2016**, *24*, 123–128. [CrossRef]

102. Verma, A.; Mehata, M.S. Controllable synthesis of silver nanoparticles using Neem leaves and their antimicrobial activity. *J. Radiat. Res. Appl. Sci.* **2016**, *9*, 109–115. [CrossRef]

103. Zhang, Y.; Cheng, X.; Zhang, Y.; Xue, X.; Fu, Y. Biosynthesis of silver nanoparticles at room temperature using aqueous aloe leaf extract and antibacterial properties. *Colloids Surf. A. Physicochem. Eng. Asp.* **2013**, *423*, 63–68. [CrossRef]

104. Sahu, N.; Soni, D.; Chandrashekhar, B.; Sarangi, B.K.; Satpute, D.; Pandey, R.A. Synthesis and characterization of silver nanoparticles using *Cynodon dactylon* leaves and assessment of their antibacterial activity. *Bioprocess Biosyst. Eng.* **2013**, *36*, 999–1004. [CrossRef]

105. Singhal, G.; Bhavesh, R.; Kasariya, K.; Sharma, A.R.; Singh, R.P. Biosynthesis of silver nanoparticles using *Ocimum sanctum* (Tulsi) leaf extract and screening its antimicrobial activity. *J. Nanopart. Res.* **2011**, *13*, 2981–2988. [CrossRef]

106. Ajitha, B.; Reddy, Y.A.K.; Reddy, P.S. Biogenic nano-scale silver particles by *Tephrosia purpurea* leaf extract and their inborn antimicrobial activity. *Spectrochim. Acta Part A Mol. Biomol. Spectrosc.* **2014**, *121*, 164–172. [CrossRef] [PubMed]

107. Logeswari, P.; Silambarasan, S.; Abraham, J. Synthesis of silver nanoparticles using plants extract and analysis of their antimicrobial property. *J. Saudi Chem. Soc.* **2015**, *19*, 311–317. [CrossRef]

108. Susanthy, D.; Santosa, S.J.; Kunarti, E.S. The Synthesis and Stability Study of Silver Nanoparticles Prepared by Using p-Aminobenzoic Acid as Reducing and Stabilizing Agent. *Indones. J. Chem.* **2018**, *18*, 421–427. [CrossRef]

109. Tomaszewska, E.; Soliwoda, K.; Kadziola, K.; Tkacz-Szczesna, B.; Celichowski, G.; Cichomski, M.; Szmaja, W.; Grobelny, J. Detection limits of DLS and UV-Vis spectroscopy in characterization of polydisperse nanoparticles colloids. *J. Nanomater.* **2013**, *2013*, 60. [CrossRef]

110. Yang, N.; Li, W.H. Mango peel extract mediated novel route for synthesis of silver nanoparticles and antibacterial application of silver nanoparticles loaded onto non-woven fabrics. *Ind. Crop. Prod.* **2013**, *48*, 81–88. [CrossRef]

111. Suriyakalaa, U.; Antony, J.J.; Suganya, S.; Siva, D.; Sukirtha, R.; Kamalakkannan, S.; Pichiah, P.T.; Achiraman, S. Hepatocurative activity of biosynthesized silver nanoparticles fabricated using *Andrographis paniculata*. *Colloids Surf. B Biointerfaces* **2013**, *102*, 189–194. [CrossRef]

112. Dipankar, C.; Murugan, S. The green synthesis, characterization and evaluation of the biological activities of silver nanoparticles synthesized from *Iresine herbstii* leaf aqueous extracts. *Colloids Surf. B Biointerfaces* **2012**, *98*, 112–119. [CrossRef] [PubMed]

113. Lee, C.Y.; Nanah, C.N.; Held, R.A.; Clark, A.R.; Huynh, U.G.; Maraskine, M.C.; Uzarski, R.L.; McCracken, J.; Sharma, A. Effect of electron donating groups on polyphenol-based antioxidant dendrimers. *Biochimie* **2015**, *111*, 125–134. [CrossRef]

114. Mittal, A.K.; Kaler, A.; Banerjee, U.C. Free Radical Scavenging and Antioxidant Activity of Silver Nanoparticles Synthesized from Flower Extract of *Rhododendron dauricum*. *Nano Biomed. Eng.* **2012**, *4*, 118–124. [CrossRef]

115. Genc, N. Biosynthesis of silver nanoparticles using *Origanum onites* extract and investigation of their antioxidant activity. *Part. Sci. Technol.* **2021**, *39*, 562–568. [CrossRef]

116. Saratale, G.D.; Saratale, R.G.; Benelli, G.; Kumar, G.; Pugazhendhi, A.; Kim, D.S.; Shin, H.S. Anti-diabetic potential of silver nanoparticles synthesized with *Argyreia nervosa* leaf extract high synergistic antibacterial activity with standard antibiotics against foodborne bacteria. *J. Clust. Sci.* **2017**, *28*, 1709–1727. [CrossRef]

117. Kokila, T.; Ramesh, P.S.; Geetha, D. Biosynthesis of silver nanoparticles from Cavendish banana peel extract and its antibacterial and free radical scavenging assay: A novel biological approach. *Appl. Nanosci.* **2015**, *5*, 911–920. [CrossRef]

118. Nayaka, S.; Chakraborty, B.; Pallavi, S.; Bhat, M.P.; Shashiraj, K.N.; Ghasti, B. Synthesis of biogenic silver nanoparticles using *Zanthoxylum rhetsa* (Roxb.) DC seed coat extract as reducing agent and in-vitro assessment of anticancer effect on A549 lung cancer cell line. *Int. J. Pharm. Res.* **2020**, *12*, 302–314.

119. Das, S.; Das, J.; Samadder, A.; Bhattacharyya, S.S.; Das, D.; Khuda-Bukhsh, A.R. Biosynthesized silver nanoparticles by ethanolic extracts of *Phytolacca decandra*, *Gelsemium sempervirens*, *Hydrastis canadensis* and *Thuja occidentalis* induce differential cytotoxicity through G2/M arrest in A375 cells. *Colloids Surf. B. Biointerfaces* **2013**, *101*, 325–336. [CrossRef]

120. Barabadi, H.; Ovais, M.; Shinwari, Z.K.; Saravanan, M. Anti-cancer green bionanomaterials: Present status and future prospects. *Green Chem. Lett. Rev.* **2017**, *10*, 285–314. [CrossRef]

121. Tinajero-Díaz, E.; Salado-Leza, D.; Gonzalez, C.; Martínez Velázquez, M.; López, Z.; Bravo-Madrigal, J.; Knauth, P.; Flores-Hernández, F.Y.; Herrera-Rodríguez, S.E.; Navarro, R.E.; et al. Green metallic nanoparticles for cancer therapy: Evaluation models and cancer applications. *Pharmaceutics* **2021**, *13*, 1719. [CrossRef]

122. Macovei, I.; Miron, A.; Gradinaru, A.C.; Aprotosoaie, A.C. Green synthesized silver nanoparticles via plant extracts as anti-melanoma agents. *Rev. Med. Chir. Soc. Med. Nat. Iasi* **2018**, *122*, 627–633.

123. González-Pedroza, M.G.; Argueta-Figueroa, L.; García-Contreras, R.; Jiménez-Martínez, Y.; Martínez-Martínez, E.; Navarro-Marchal, S.A.; Marchal, J.A.; Morales-Luckie, R.A.; Boulaiz, H. Silver nanoparticles from *Annona muricata* peel and leaf extracts as a potential potent, biocompatible and low cost antitumor tool. *Nanomaterials* **2021**, *11*, 1273. [CrossRef] [PubMed]

124. Thakur, S.; Mohan, G.K. Green synthesis of silver nanoparticles of boswellic acid, and its in vitro anticancer activity. *Int. J. Pharma. Bio. Sci.* **2019**, *10*, 92–100.

125. Islam, M.A.; Jacob, M.V.; Antunes, E. A critical review on silver nanoparticles: From synthesis and applications to its mitigation through low-cost adsorption by biochar. *J. Environ. Manag.* **2021**, *281*, 111918. [CrossRef] [PubMed]

126. Chandra Pal, H.; Marchiony Hunt, K.; Diamond, A.; A Elmets, C.; Afaq, F. Phytochemicals for the management of melanoma. *Mini. Rev. Med. Chem.* **2016**, *16*, 953–979. [CrossRef]

127. Thaichinda, S.; Tancharoen, S.; Kanekura, T.; Higashi, Y.; Dararat, P.; Kikuchi, K.; Nararatwanchai, T. *Pinus maritima* Extract Induces Apoptosis in Human Malignant Melanoma Cells via ROS/Caspase-3 Signaling. *Nat. Prod. Commun.* **2020**, *15*, 1934578X20926889. [CrossRef]

128. Vanlalveni, C.; Lallianrawna, S.; Biswas, A.; Selvaraj, M.; Changmai, B.; Rokhum, S.L. Green synthesis of silver nanoparticles using plant extracts and their antimicrobial activities: A review of recent literature. *RSC Adv.* **2021**, *11*, 2804–2837. [CrossRef]

129. Liu, S.; Zhang, Q.; Li, H.; Qiu, Z.; Yu, Y. Comparative Assessment of the Antibacterial Efficacies and Mechanisms of Different Tea Extracts. *Foods* **2022**, *11*, 620. [CrossRef] [PubMed]

130. Ali, K.; Ahmed, B.; Dwivedi, S.; Saquib, Q.; Al-Khedhairy, A.A.; Musarrat, J. Microwave accelerated green synthesis of stable silver nanoparticles with *Eucalyptus globulus* leaf extract and their antibacterial and antibiofilm activity on clinical isolates. *PLoS ONE* **2015**, *10*, e0131178. [CrossRef] [PubMed]

131. He, Y.; Wei, F.; Ma, Z.; Zhang, H.; Yang, Q.; Yao, B.; Huang, Z.; Li, J.; Zeng, C.; Zhang, Q. Green synthesis of silver nanoparticles using seed extract of *Alpinia katsumadai*, and their antioxidant, cytotoxicity, and antibacterial activities. *RSC Adv.* **2017**, *7*, 39842–39851. [CrossRef]